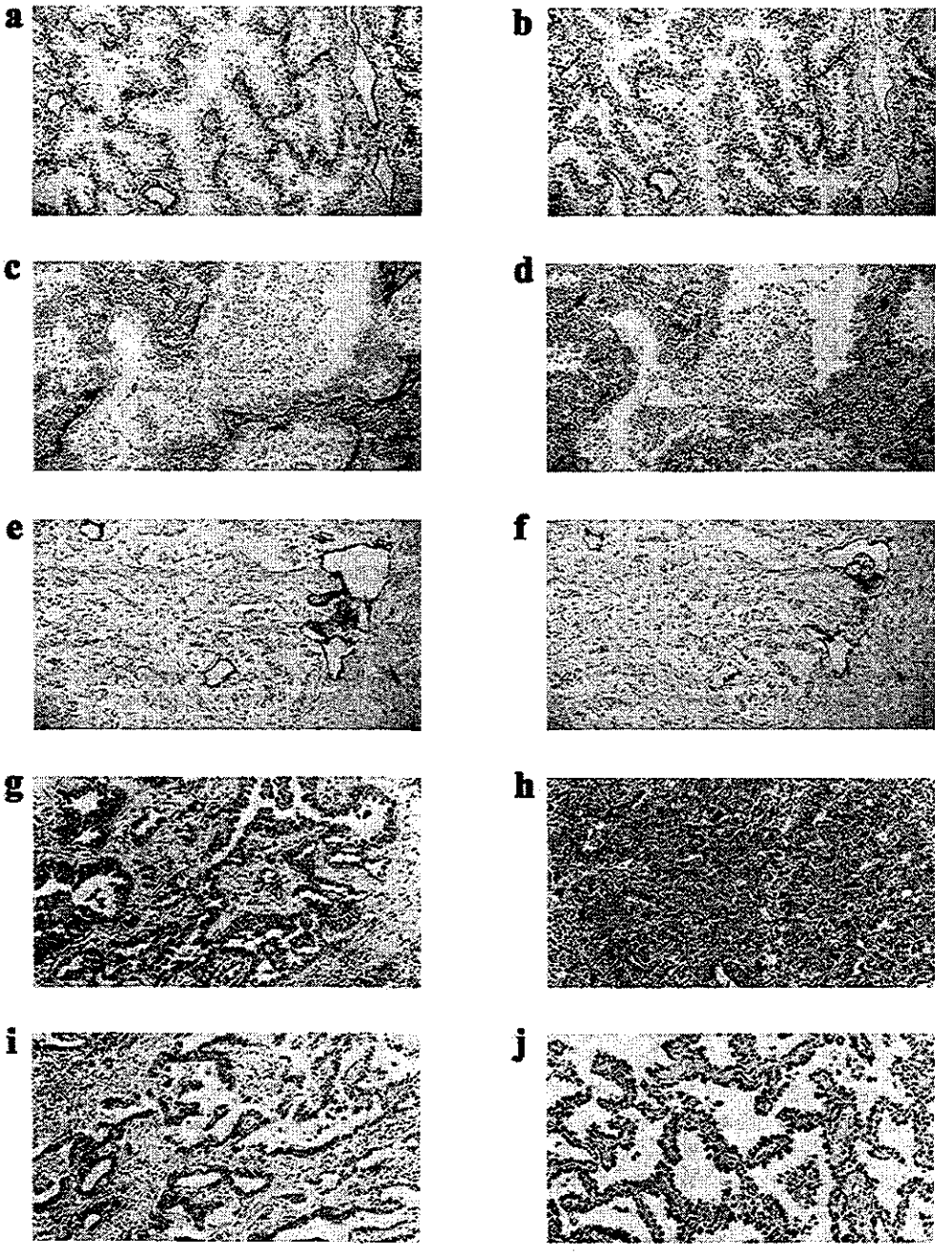

Fig. 2. (a–f) Representative immunohistochemical findings of type IV collagen (a, c and e) and laminin (b, d and f), and as for grades of basement membrane preservation, (a and b) grade A shows almost total preservation of both BM components along cancer cell nests (BAC type of growth pattern), (c and d) grade B reveals well-preserved type IV collagen, but not laminin (papillary type), and (e and f) grade C shows the total lack of BM components around cancer cells nests in the desmoplastic area. Original magnification: × 50 (g–j) representative immunohistochemical findings of MMP-2 (g), -9 (h) and -14 (i), and TIMP-2 (j). Cancer cells proliferating in the papillary type of growth pattern are strongly positive for MMP-2 (g) and MMP-14 (i) (different case), and solid type cancer cells are positive for MMP -9 (h). BAC type cancer cells show an apparent positive reaction for TIMP-2 (j). Original magnification: × 50.

Statistical analyses

To estimate the correlation between the growth/fibrosis pattern, BM antigens and expression of MMPs and TIMP-2, the chi-square test and the Kruskal–Wallis test were used. The Kaplan–Meier method was used to estimate overall survival time, and differences were analyzed using the log-rank test based on the clinicopathologic parameters of clinical stage, lymph node metastasis, histologic subtypes, expression of MMP-2 and TIMP-2, and the existence of fibrotic foci. Regarding the expression of MMP-2 and TIMP-2, the

relationship between BM preservation and the degree of MMP-2 or TIMP-2 expression was found to be statistically significant by the Kruskal–Wallis' test as shown in Fig. 4 (MV±SD of MMP-2 and TIMP-2 expressions were 11.5±1.5 and 21.9±1.7%, respectively). Therefore, we subdivided the high expression group of each protein and analyzed the survival curves for statistical differences, i.e., the high expression group of MMP-2 when its positive cell ratio was greater than 10% in at least one of the growth pattern foci examined, and the high expression group of TIMP-2 if the positive cell ratio was greater than 20% in all growth pattern foci examined. Analyzing the relationship between the presence of fibrotic foci and overall survival time, we considered the desmoplastic type if there was a coexistence between the desmoplastic and the collapse type in each case. For uni- and multivariate analyses of the parameters described above, we used the Cox proportional hazards model. Probability values of less than 0.05 were regarded as significant in all analyses.

Results

Histologic findings

The frequency of growth and fibrosis patterns in each histologic subtype of 76 lung adenocarcinomas is summarized in Table 2. The 76 adenocarcinoma lesions examined consisted of 6 non-mucinous BACs, including one with invasive growth, 49 papillary/acinar adenocarcinomas, and 21 solid adenocarcinomas. We subdivided the 76 lesions into 147 foci according to the predominant growth pattern of the cancer cells and the occurrence of fibrosis; there were 19 foci of BAC (Fig. 1a, 12.9%), 53 foci of papillary (Fig. 1b)/acinar adenocarcinomas (Fig. 1c) (36.1%), and 31 foci of solid growth patterns (Fig. 1d) (21.1%), as well as 9 foci of the collapse type (Figs. 1e and g) (6.1%) and 35 foci of the desmoplastic type of stromal fibrosis (Figs. 1f and h) (23.8%). The papillary/acinar and solid subtypes of adenocarcinoma lesions were frequently associated with other growth patterns (36.7% and 28.6%, respectively). All desmoplastic foci, except one focus in the BAC subtype, were found in the papillary/acinar and solid subtypes, and the incidence for three histologic subtypes was 16.7% in BAC, 42.9% in papillary/acinar, and 61.9% in solid subtypes, respectively.

The relationship between growth pattern/fibrosis type and grade of basement membrane antigens preservation

The grades for BM antigens preservation in each growth pattern or fibrosis type are summarized in Table 3. Grade A or B of BM preservation (Figs. 2a–d), i.e., a preservation rate greater than 90% for either laminin or type IV collagen, or for both of these types means that the state of the BM components was well preserved, and this applied to 94.7% of BAC growth patterns, to 24.5% of papillary/acinar, and to 16.1% of solid growth patterns. By contrast, grade C of BM preservation (Figs. 2e and f), i.e., a preservation rate of less than 90% for both type IV collagen and laminin was considered a poorly preserved state of BM antigens, noted in more than 75.5% of papillary/acinar and solid growth patterns. All foci of the desmoplastic fibrosis and 55.6% of the foci of the collapse type were assigned to grade C, and, characteristically, the BM completely disappeared in foci in case of desmoplastic fibrosis. Destruction of BM structures significantly correlated with the growth and fibrosis patterns (Table 3, $p<0.01$).

Table 3. Relationship between growth/fibrosis pattern and grade of basement membrane antigens preservation

	Grades of BM preservation[a]			Total
	A	B	C	
Growth pattern				
BAC	8 (42.1)	10 (52.6)	1 (5.3)*	19
Papillary/acinar	1 (1.9)	12 (22.6)	40 (75.5)	53
Solid	0 (0)	5 (16.1)	26 (83.9)	31
Total	9	27	67	103
Fibrosis pattern				
Collapse	3 (33.3)	1 (11.1)	5 (55.6)**	9
Desmoplastic	0 (0)	0 (0)	35 (100)	35
Total	3	1	40	44

[a]Grade A or C means that both laminin and type IV collagen were preserved more or less than 90% around cancer cell nests, respectively, and grade B corresponds in cases in which either laminin or type IV collagen is preserved more than 90%. The number in parentheses expresses each percentage.

*$P<0.01$: vs. papillary/acinar and solid type (chi-square test).

**$P<0.01$: vs. desmoplastic type (chi-square test).

The relationship between growth pattern/fibrosis type and expressions of MMPs and TIMP-2

Representative findings of MMP-2, -9 and -14, and TIMP-2 expressions in cancer cells are shown in Figs. 2(g–j). The immunoreaction products for MMPs and TIMP-2 were finely granular and localized in the cytoplasm of tumor cells. In the desmoplastic foci, cancer cells occasionally showed strong immunoreactivity for MMPs and TIMP-2 antigens, but this number was frequently so small that we had to exclude it from the evaluation. Stromal fibroblasts in desmoplastic

fibrotic foci also showed immunohistochemical positivity for the antigens (data not shown). Examining the relationship between the growth pattern of cancer cells and MMPs or TIMP-2 expression in cancer cells, the expression of TIMP-2 correlated well with the growth pattern, i.e., the TIMP-2-positive cell ratio was lower in solid and papillary/acinar growth patterns (12.5±2.2 and 21.9±1.4%, respectively) than that of BAC growth pattern (39.0±4.0%) ($p<0.001$) (Fig. 3). However, no significant correlation was found between the expression of MMPs and each growth pattern (data not shown).

Regarding the relationship between the grade of BM preservation and the expression of MMPs and TIMP-2, MMP-2 correlated reversely with the grade of BM preservation ($p<0.05$, Fig. 4). By contrast, TIMP-2 expression correlated positively with the BM preservation ($p<0.05$), while MMP-9 and -14 expressions did not correlate for whole lesion foci (Fig. 4). In addition, the expression of MMP-2 was significantly higher in poorly preserved foci of BM antigens (grade C of BM preservation; 14.4±1.1%) than that in well-preserved foci (grades A and B; 9.7±3.7% and 10.2±2.3%, respectively) ($p<0.05$), while TIMP-2 expression was significantly lower in poorly preserved foci (17.6±1.0%) of BM antigen than that in well-preserved foci (grades A and B; 34.8±3.8 and 24.4±2.7%, respectively) ($p<0.05$).

The prognostic values of the expression of MMPs/TIMP-2, growth pattern, fibrosis type, and other clinicopathologic parameters

From the findings that the degree of BM preservation correlated well with the expression status of MMP-2 and TIMP-2 antigens (Fig. 4), we also subdivided each case into high and low expression groups (MMP-2–10%; TIMP-2–20%), because these values were equivalent to the mean value minus standard deviation (MV-SD) of MMP-2 (10.0%) and TIMP-2 (20.2%) positive ratios. If more than two foci were examined for MMP-2 and TIMP-2 expression in each case, the mean value of these parameters was used as the representative for the individual case, and the respective prognostic value of these antigen expressions was then evaluated statistically.

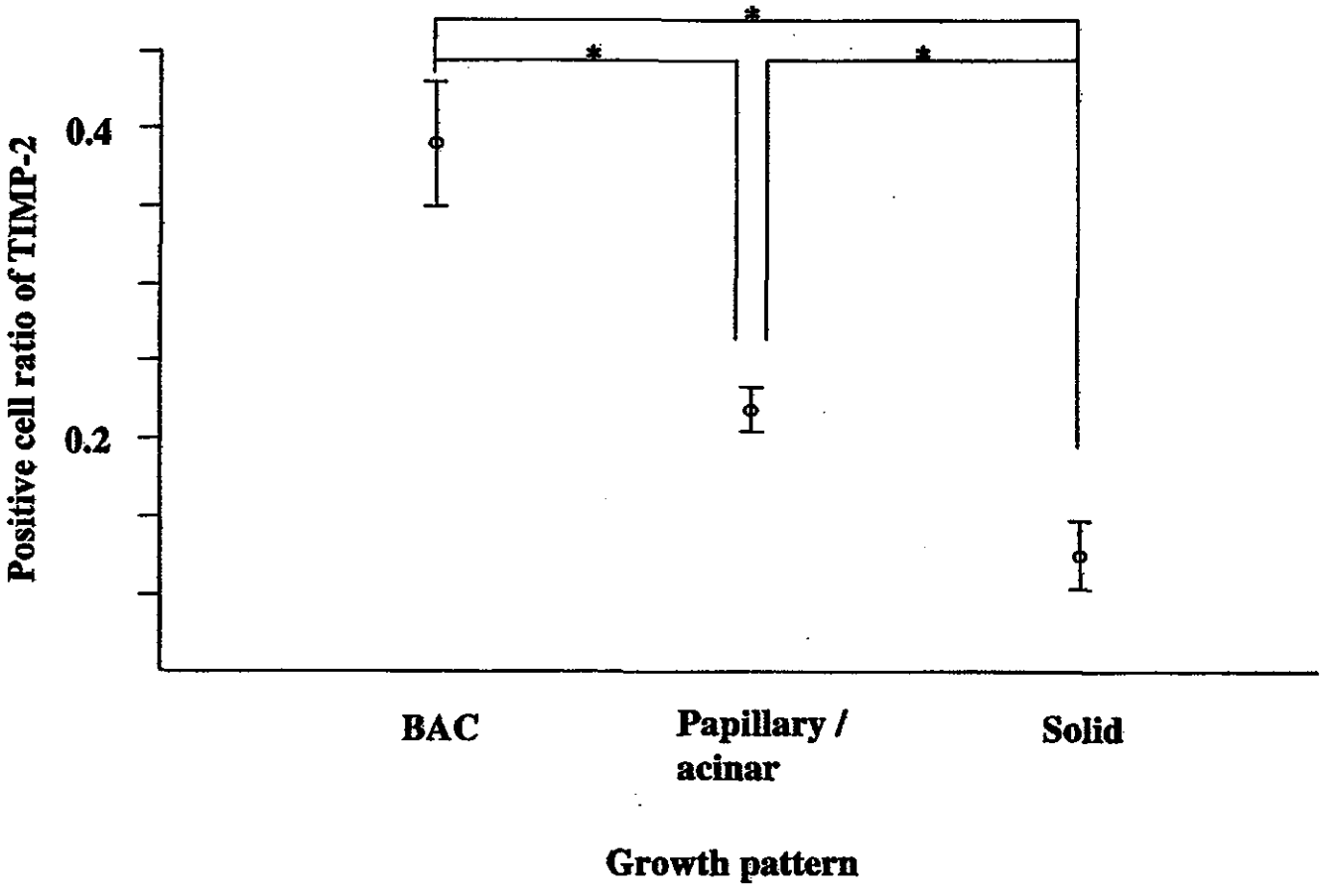

Fig. 3. Relationship between growth pattern and TIMP-2 expression. There are significant differences in positive cell ratio of TIMP-2 among three growth patterns. TIMP-2 expression is highest in BAC type cancer cells and lowest in solid type cancer cells. *$p<0.001$ (Kruskal–Wallis' test and Mann–Whitney's U test).

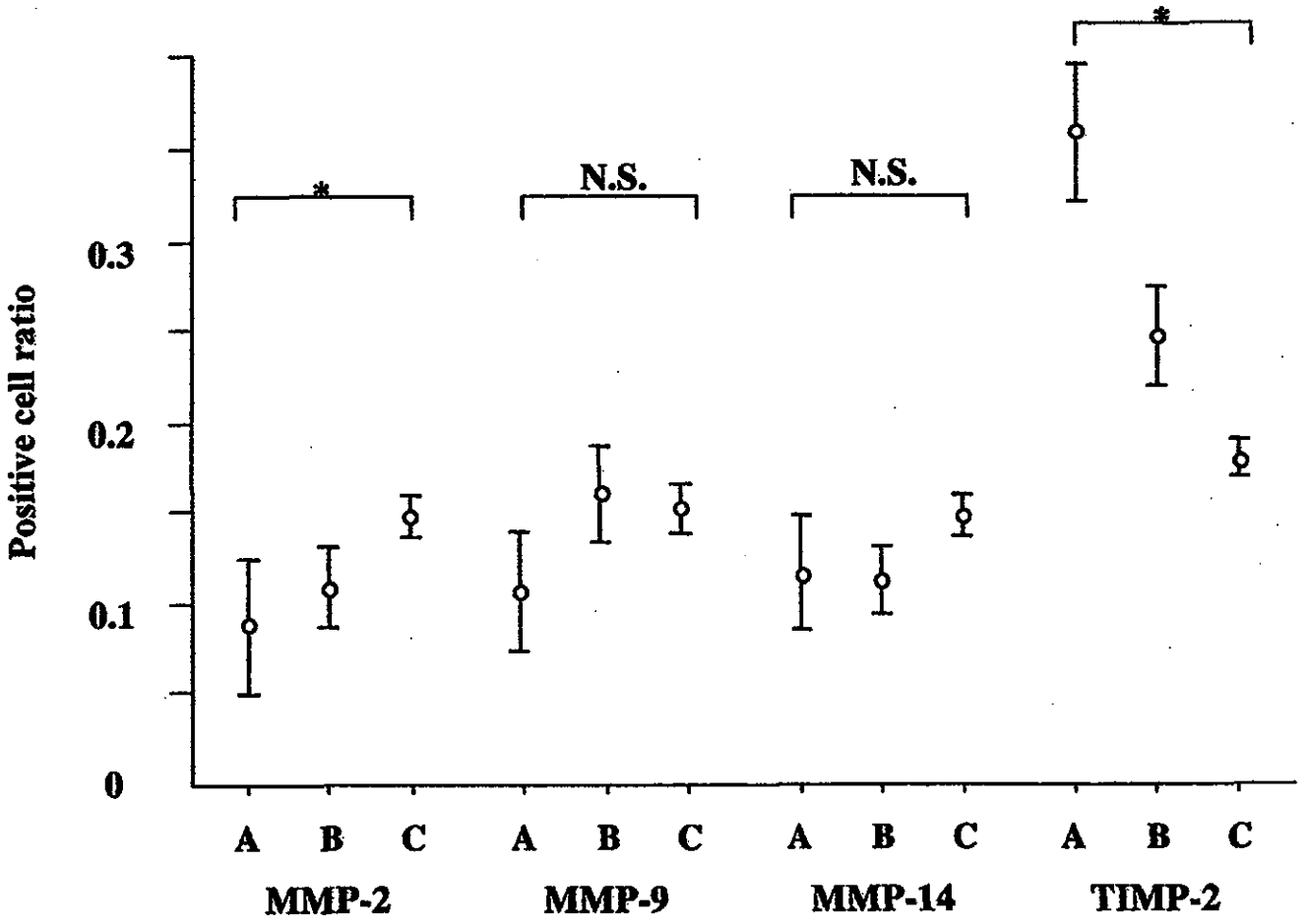

Fig. 4. Relationship between the grade of BM antigen preservation and expression of MMPs and TIMP-2. Grade A or C means that both laminin and type IV collagen were preserved more or less than 60% around cancer cell nests, respectively, and grade B corresponds to cases in which either laminin or type IV collagen is preserved more than 60%. MMP-2 expression is significantly higher in grade C foci of BM preservation than in grade A foci, while the relationship between TIMP-2 expression and grade of BM preservation is reverse. $^{*}p<0.05$ (Kruskal–Wallis' test), N.S.; not significant.

The results of statistical survival analyses for clinicopathologic variables and immunohistochemical parameters are summarized in Figs. 5a–c and Table 4. Thirty-seven cases were categorized in the high expression group of MMP-2, and 22 cases were assigned to the high expression group of TIMP-2. Using the Kaplan–Meier method, the prognosis of patients with high expression of TIMP-2 was significantly better than that for the low expression group ($p=0.0003$, Fig. 5a), while the MMP-2 expression status did not correlate with prognosis (data not shown). Analyses of the relationship between survival rates and growth patterns also revealed that the prognosis of the patients with papillary/acinar or solid subtypes was significantly worse than that of the patients with the BAC subtype ($p=0.0084$, Fig. 5b). The survival rate for patients without desmoplastic fibrosis was also significantly better than for those with desmoplastic fibrosis ($p=0.018$, Fig. 5c), while there was no significant correlation between collapse fibrosis and prognosis.

Cox univariate regression analyses identified the pathologic stage ($p=0.0004$), nodal metastasis ($p=0.0031$), high expression of TIMP-2 ($p=0.026$), the

Fig. 5. Kaplan–Meier survival curves for all patients with respect to TIMP-2 expression (a), histologic subtypes (b), and presence of desmoplastic fibrosis (c). Survival curves are shown for patients with high/low expression of TIMP-2 (a), for each histologic subtype such as BAC, papillary/acinar and solid adenocarcinomas (b), and for those with or without desmoplastic fibrosis (c). The prognosis of the TIMP-2 high expression group was significantly better than that of the low expression group. The prognosis of the patients with papillary/acinar and solid types is significantly poorer than that of the patients with BAC type (a). There is a significant difference between patients with and without the focus of desmoplastic fibrosis (b). *Logrank test.

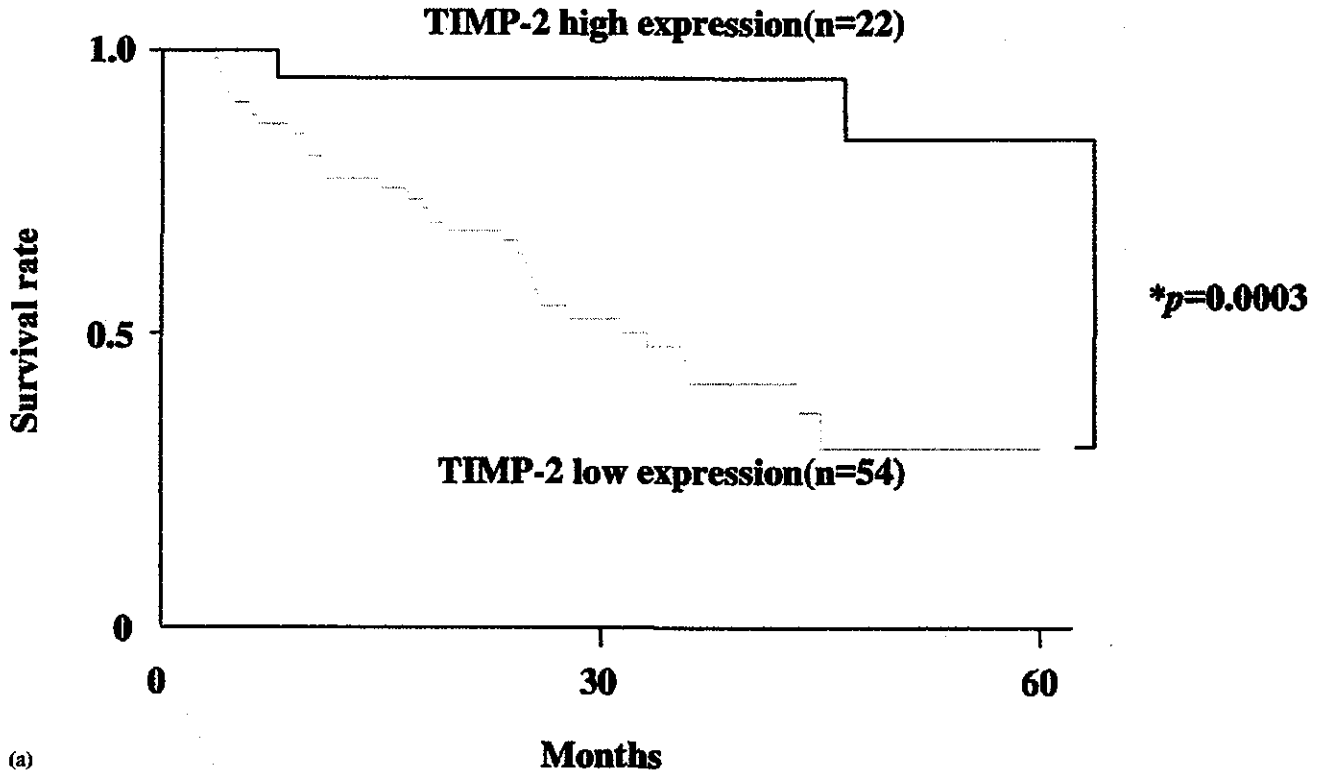
TIMP-2 high expression(n=22)
1.0
0.5
0
Survival rate
*p=0.0003
TIMP-2 low expression(n=54)
0
30
60
Months

(a)

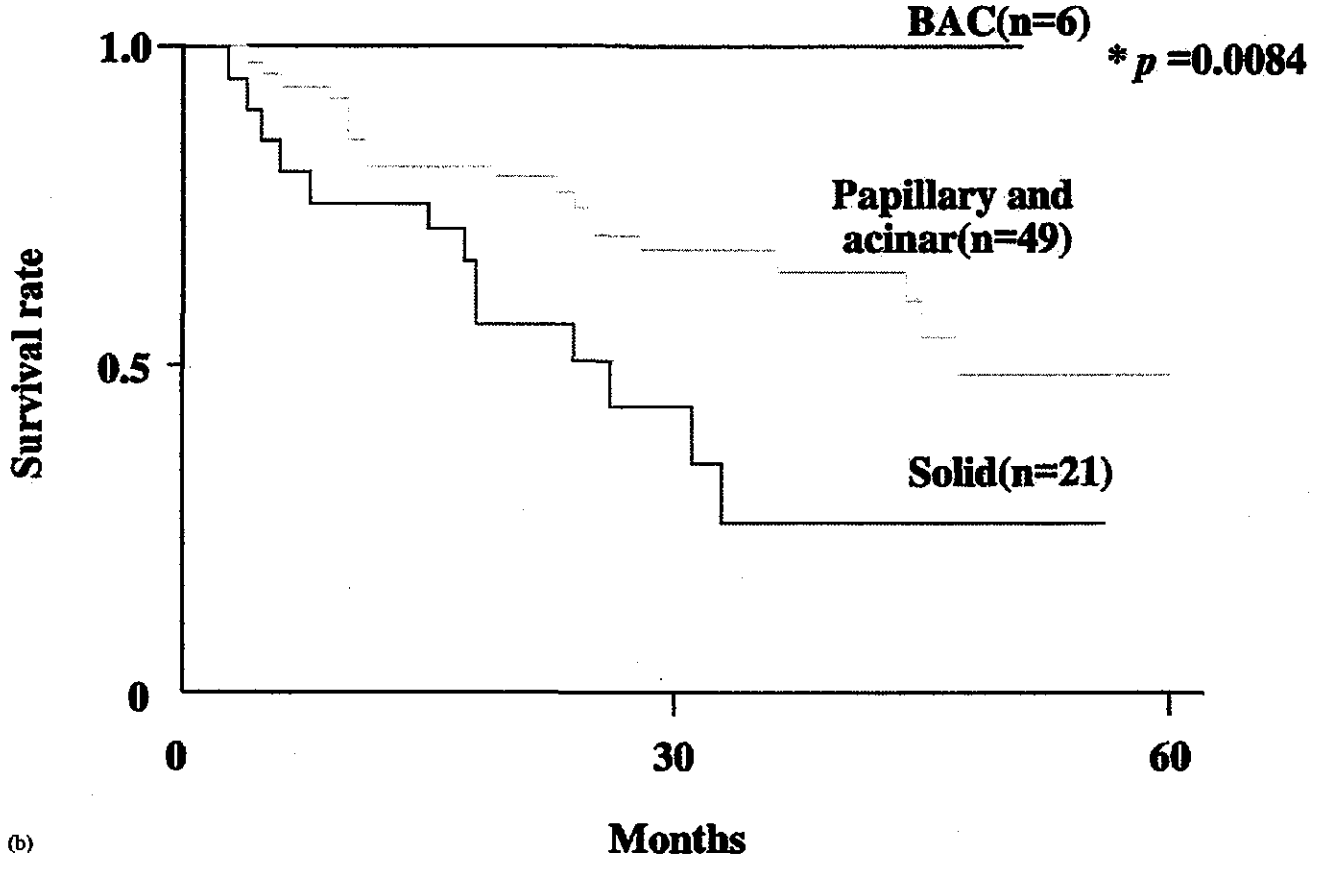
BAC(n=6)
* p =0.0084
1.0
Papillary and
acinar(n=49)
0.5
Solid(n=21)
0
Survival rate
0
30
60
Months

(b)

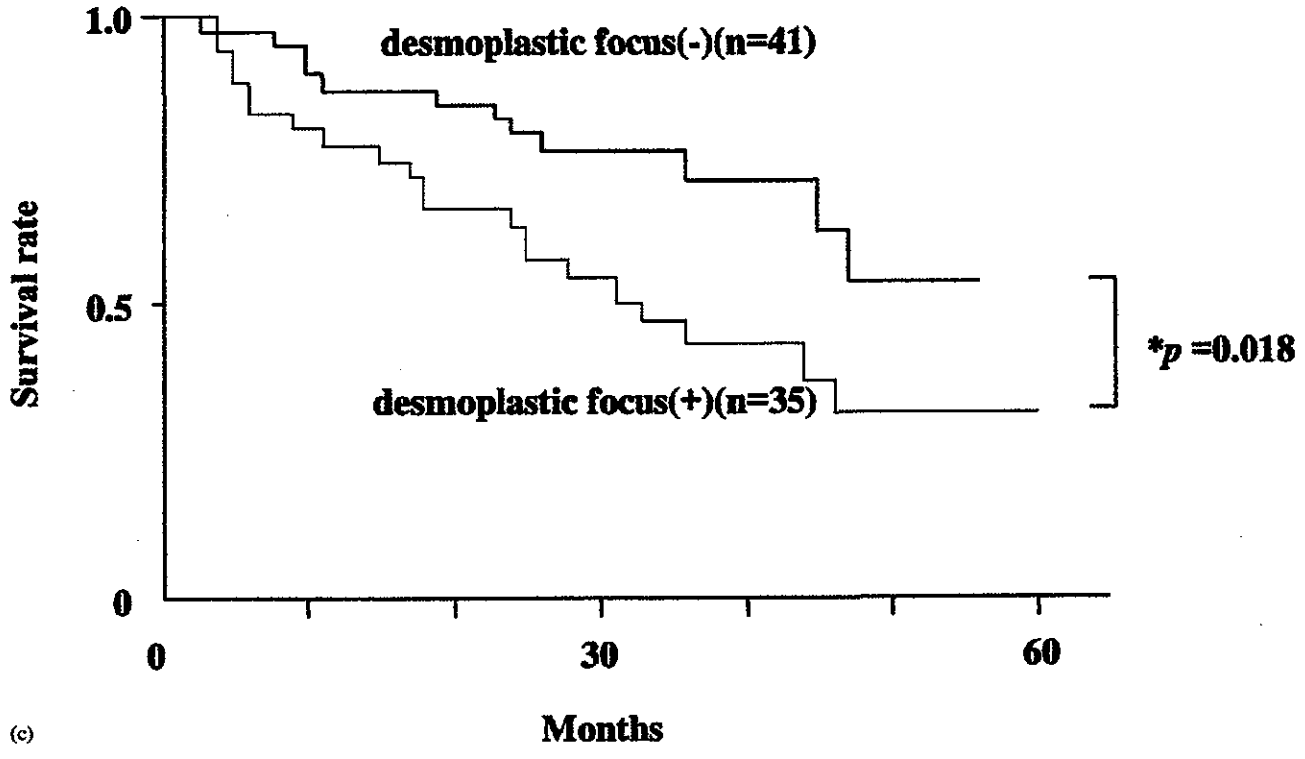

Fig. 5 (*continued*).

existence of desmoplastic fibrosis ($p=0.0216$), and the histologic subtype ($p=0.0013$) as significant prognostic predictors (Table 4). Multivariate analyses revealed that high expression of TIMP-2 and the pathologic stage were independent prognostic factors ($p=0.0165$ and 0.0078, respectively, Table 4).

Discussion

Human peripheral lung adenocarcinoma is histologically heterogeneous [11,33]. In the new classification of lung cancer proposed by WHO/IASLC (International Association for the Study of Lung Cancer) in 1999 [33], lung adenocarcinomas are subdivided into four subtypes representing a mixture of four major growth patterns: BAC, acinar, papillary, and solid patterns. Our study shows that heterogeneous properties occur not only in histopathology, but also in the immunoreactivity for BM antigens, MMPs and TIMP-2 within 147 foci showing four major growth patterns and collapsed or desmoplastic fibrosis, observed in 76 Japanese lung adenocarcinomas. The BM was well preserved in foci of BAC growth pattern, where TIMP-2 expression in cancer cells was enhanced, while MMP-2 expression was suppressed. BM antigens, type IV collagen, and laminin disappeared in desmoplastic foci, and desmoplastic alteration of stroma was more frequently observed in non-BAC lesions. In addition to better prognostic parameters such as the BAC subtype with or without invasive growth and pathologic stage, patients affected by adenocarcinomas with high expression of TIMP-2 had a better survival rate than those with low TIMP-2 expression. Conversely, nodal involvement and stromal desmoplasia were poor prognostic factors. The high expression of TIMP-2 in cancer cells, as well as the pathologic stage, was found to be independent of beneficial effects for survival time as determined by a multivariate analysis. To our knowledge, this report is the first to suggest that histologic heterogeneity of lung adenocarcinoma partly correlates with the cancer cell-stromal interaction, probably because of the preserved structure and function of BM caused by high expression of TIMP-2 in cancer tissue.

Distribution of BM antigens and molecular and immunohistochemical expression of MMPs and TIMPs have been observed in various human tumors [4,5,7,12,13,16], including lung adenocarcinomas [8,10,14,21,23], and the enhanced expression of MMPs has been assumed to be related to cancer cell invasiveness associated with destruction of BM around cancer cells. Previous studies [14,23] showed that BM antigens were well preserved in the BAC lesion without stromal fibrosis or scar formation compared with other types of adenocarcinoma, and the desmoplastic reaction of

Table 4. Univariate and multivariate analyses with Cox's proportional hazards model

Variables	Univariate			Multivariate		
	Hazards ratio	95% CI[a]	*p*	Hazards ratio	95% CI[a]	*p*
Pathological stage	1.422	1.168–1.731	0.0004	1.560	1.124–2.165	0.0078
Lymph node metastasis	1.692	1.194–2.398	0.0031	0.641	0.351–1.170	0.1475
Histologic subtype	2.952	1.526–5.709	0.0013	1.941	0.921–4.093	0.0812
Desmoplastic focus	2.316	1.131–4.743	0.0216	1.882	0.898–3.947	0.0941
MMP-2 high expression	1.314	0.652–2.648	0.4456	1.585	0.744–3.373	0.2323
TIMP-2 high expression	0.110	0.026–0.464	0.026	0.155	0.034–0.712	0.0165

[a]CI: confidence interval.

stroma is closely associated with the enhanced expression of MMPs, particularly of MMP-2, and with an extensive destruction of BM. However, concomitant expression and the pathophysiologic role of TIMPs are controversial. In lung adenocarcinoma, Kitamura et al. [10] showed that TIMP-2 expression was strongly associated with the presence of central sclerosis, and Kumaki et al. [14] also reported that TIMP-2 was co-expressed with MMP-2 by cancer cells in invasive areas. They suggested that TIMP-2 accumulation in cancer stroma following its expression by cancer cells and stromal cells might participate in stromal fibrosis, but not directly in the regulation of cancer cell invasiveness. By contrast, Giannelli et al. [4] reported that up-regulation of MMP-2 and down-regulation of TIMP-2 in cancer cells were observed not only in primary lesions of hepatocellular carcinoma patients with metastasis, but also in their metastatic foci. As the immunohistochemical expression of MMPs and TIMP-2 in cancer cells varied in intensity, and distribution was heterogeneous even within an individual lung adenocarcinoma lesion, we considered it important to examine and assess these labeling indices in each focus of the four major growth patterns. We found that the destruction of the BM correlated well with the down-regulation of TIMP-2 and up-regulation of MMP-2 among the MMPs examined, and was frequent in non-BAC foci that were significantly associated with low expression of TIMP-2, but not with high expression of MMP-2. These results suggest that the reduced balance of the TIMP-2/MMP-2 expression ratio in cancer cells plays a critical role in the disruption of the BM in lung adenocarcinoma, but other MMPs such as MMP-3, -7 and -11 [8,20] may also contribute to this. As TIMP-2 expression in cancer cells was closely related to each growth pattern, the decreased expression of TIMP-2 may be regarded as the most important factor involved in BM destruction of lung adenocarcinomas. In fact, TIMP-2 has been shown to have a broader and stronger inhibitory effect on MMPs than TIMP-1 [9,27].

In the Kaplan–Meier and Cox univariate regression analyses, the histologic subtype, the existence of desmoplastic fibrosis, the pathologic stage, and nodal metastasis showed a significant correlation with the survival rate of lung adenocarcinoma patients, and these results are comparable to those reported in previous studies [11,22,29,34]. In addition, the expression of TIMP-2 was also a prognostic factor of lung adenocarcinoma. The prognosis of patients with high expression of TIMP-2 in all foci examined was apparently better than that of the patients with low expression of TIMP-2. In the multivariate regression analyses, high expression of TIMP-2, as well as the pathologic stage, was identified to be an independent prognostic factor. Therefore, the evaluation of TIMP-2 expression in each growth pattern focus is useful for predicting the prognosis.

In summary, lung adenocarcinoma is histopathologically and immunohistochemically heterogeneous, based on the growth pattern of cancer cells and distribution of several antigens, including constituents of BM, MMPs and TIMP-2, but the growth pattern of lung adenocarcinoma cells correlates well with the disruption or preservation of the BM components and the expression of TIMP-2. High expression of TIMP-2 may be one determinant of the histologic subtypes and may constitute an important prognostic factor in lung adenocarcinoma.

Acknowledgements

We thank Hiroshi Fujii for preparing the tissue sections and Mariko Ohara for providing assistance regarding the English language.

References

[1] E. Campo, M.J. Merino, L. Liotta, R. Neumann, W. Stetler-Stevenson, Distribution of the 72-kd type IV collagenase in nonneoplastic and neoplastic thyroid tissue, Hum. Pathol. 23 (1992) 1395–1401.

[2] E. Campo, M.J. Merino, F.A. Tavassoli, A.S. Charonis, W.G. Stetler-Stevenson, L.A. Liotta, Evaluation of basement membrane components and the 72 kDa type IV

collagenase in serous tumors of the ovary, Am. J. Surg. Pathol. 16 (1992) 500–507.
[3] M.R. Clarke, R.J. Landreneau, S.D. Finkelstein, T.T. Wu, P. Ohori, S.A. Yousem, Extracellular matrix expression in metastasizing and nonmetastasizing adenocarcinomas of the lung, Hum. Pathol. 28 (1997) 54–59.
[4] G. Giannelli, C. Bergamini, F. Marinosci, et al., Clinical role of MMP-2/TIMP-2 imbalance in hepatocellular carcinoma, Int. J. Cancer 97 (2002) 425–431.
[5] W.F. Grigioni, A. D'Errico, C. Fortunato, et al., Prognosis of gastric carcinoma revealed by interactions between tumor cells and basement membrane, Mod. Pathol. 7 (1994) 220–225.
[6] M. Higashiyama, O. Doi, K. Kodama, H. Yokouchi, R. Tateishi, Cathepsin B expression in tumour cells and laminin distribution in pulmonary adenocarcinoma, J. Clin. Pathol. 46 (1993) 18–22.
[7] E.E. Ioachim, S.E. Athanassiadou, S. Kamina, K. Carassavoglou, N.J. Agnantis, Matrix metalloproteinase expression in human breast cancer: an immunohistochemical study including correlation with cathepsin D, type IV collagen, laminin, fibronectin, EGFR, c-erbB-2 oncoprotein, p53, steroid receptors status and proliferative indices, Anticancer Res. 18 (1998) 1665–1670.
[8] N. Kawano, H. Osawa, T. Ito, et al., Expression of gelatinase A, tissue inhibitor of metalloproteinases-2, matrilysin, and trypsin(ogen) in lung neoplasms: an immunohistochemical study, Hum. Pathol. 28 (1997) 613–622.
[9] T. Kinoshita, H. Sato, T. Takino, M. Itoh, T. Akizawa, M. Seiki, Processing of a precursor of 72-kilodalton type IV collagenase/gelatinase A by a recombinant membrane-type 1 matrix metalloproteinase, Cancer Res. 56 (1996) 2535–2538.
[10] H. Kitamura, Y. Oosawa, N. Kawano, et al., Basement membrane patterns, gelatinase A and tissue inhibitor of metalloproteinase-2 expressions, and stromal fibrosis during the development of peripheral lung adenocarcinoma, Hum. Pathol. 30 (1999) 331–338.
[11] T. Koga, S. Hashimoto, K. Sugio, et al., Clinicopathological and molecular evidence indicating the independence of bronchioloalveolar components from other subtypes of human peripheral lung adenocarcinoma, Clin. Cancer Res. 7 (2001) 1730–1738.
[12] T. Koshiba, R. Hosotani, M. Wada, et al., Detection of matrix metalloproteinase activity in human pancreatic cancer, Surg. Today 27 (1997) 302–304.
[13] T. Krecicki, M. Zalesska-Krecicka, M. Jelen, T. Szkudlarek, M. Horobiowska, Expression of type IV collagen and matrix metalloproteinase-2 (type IV collagenase) in relation to nodal status in laryngeal cancer, Clin. Otolaryngol. 26 (2001) 469–472.
[14] F. Kumaki, K. Matsui, T. Kawai, et al., Expression of matrix metalloproteinases in invasive pulmonary adenocarcinoma with bronchioloalveolar component and atypical adenomatous hyperplasia, Am. J. Pathol. 159 (2001) 2125–2135.
[15] A.T. Levy, V. Cioce, M.E. Sobel, et al., Increased expression of the Mr 72,000 type IV collagenase in human colonic adenocarcinoma, Cancer Res. 51 (1991) 439–444.
[16] H. Maeta, S. Ohgi, T. Terada, Protein expression of matrix metalloproteinases 2 and 9 and tissue inhibitors of metalloproteinase 1 and 2 in papillary thyroid carcinomas, Virchows Arch. 438 (2001) 121–128.
[17] P. Mignatti, D.B. Rifkin, Biology and biochemistry of proteinases in tumor invasion, Physiol. Rev. 73 (1993) 161–195.
[18] C. Monteagudo, M.J. Merino, J. San-Juan, L.A. Liotta, W.G. Stetler-Stevenson, Immunohistochemical distribution of type IV collagenase in normal, benign and malignant breast tissue, Am. J. Pathol. 136 (1990) 585–592.
[19] H. Nakagawa, S. Yagihashi, Expression of type IV collagen and its degrading enzymes in squamous cell carcinoma of lung, Jpn. J. Cancer Res. 85 (1994) 934–938.
[20] B. Nawrocki, M. Polette, V. Marchand, et al., Expression of matrix metalloproteinases and their inhibitors in human bronchopulmonary carcinomas: quantificative and morphological analyses, Int. J. Cancer 72 (1997) 556–564.
[21] T. Nishino, T. Ishida, T. Oka, K. Yasumoto, K. Sugimachi, Prognostic significance of laminin in adenocarcinoma of the lung, J. Surg. Oncol. 43 (1990) 214–218.
[22] M. Noguchi, A. Morikawa, M. Kawasaki, et al., Small adenocarcinoma of the lung, Histologic characteristics and prognosis, Cancer 75 (1995) 2844–2852.
[23] N.P. Ohori, S.A. Yousem, J. Griffin, et al., Comparison of extracellular matrix antigens in subtypes of bronchioloalveolar carcinoma and conventional pulmonary adenocarcinoma. An immunohistochemical study, Am. J. Surg. Pathol. 16 (1992) 675–686.
[24] P. Paakko, J. Risteli, L. Risteli, H. Autio-Harmainen, Immunohistochemical evidence that lung carcinomas grow on alveolar basement membranes, Am. J. Surg. Pathol. 14 (1990) 464–473.
[25] R. Poulsom, M. Pignatelli, W.G. Stetler-Stevenson, et al., Stromal expression of 72 kda type IV collagenase (MMP-2) and TIMP-2 mRNAs in colorectal neoplasia, Am. J. Pathol. 141 (1992) 389–396.
[26] Y. Shimosato, A. Suzuki, T. Hashimoto, et al., Prognostic implications of fibrotic focus (scar) in small peripheral lung cancers, Am. J. Surg. Pathol. 4 (1980) 365–373.
[27] W.G. Stetler-Stevenson, H.C. Krutzsch, L.A. Liotta, Tissue inhibitor of metalloproteinase (TIMB-2), A new member of the metalloproteinase inhibitor family, J. Biol. Chem. 264 (1989) 17374–17378.
[28] N. Sukoh, S. Abe, I. Nakajima, et al., Immunohistochemical distributions of cathepsin B and basement membrane antigens in human lung adenocarcinoma: association with invasion and metastasis, Virchows Arch. 424 (1994) 33–38.
[29] K. Suzuki, T. Yokose, J. Yoshida, et al., Prognostic significance of the size of central fibrosis in peripheral adenocarcinoma of the lung, Ann. Thorac. Surg. 69 (2000) 893–897.

[30] The Japan Lung Cancer Society, General Rule for Clinical and Pathological Record of Lung Cancer, 5th Edition, Kanehara Publications, Tokyo, 1999.
[31] W.D. Travis, L.B. Travis, S.S. Devesa, Lung cancer (published erratum appears in Cancer 75(12) (1995) 2979, Cancer 75 (1995) 191–202.
[32] Union Internationale Contre le Cancer, TNM Classification of Malignant Tumors, 5th Edition, Springer, Berlin, 1997.
[33] WHO, International histological classification of tumors, Histological Typing of Lung and Pleural Tumors, 3rd Edition, 1999.
[34] T. Yokose, K. Suzuki, K. Nagai, Y. Nishiwaki, S. Sasaki, A. Ochiai, Favorable and unfavorable morphological prognostic factors in peripheral adenocarcinoma of the lung 3 cm or less in diameter, Lung Cancer 29 (2000) 179–188.

Essential Role of PDGFRα-p70S6K Signaling in Mesenchymal Cells During Therapeutic and Tumor Angiogenesis In Vivo

Role of PDGFRα During Angiogenesis

Norifumi Tsutsumi, Yoshikazu Yonemitsu, Yasunori Shikada, Mitsuho Onimaru, Mitsugu Tanii, Shinji Okano, Kazuhiro Kaneko, Mamoru Hasegawa, Makoto Hashizume, Yoshihiko Maehara, Katsuo Sueishi

Abstract—Discovery of the common and ubiquitous molecular targets for the disruption of angiogenesis, that are independent of the characteristics of malignant tumors, is desired to develop the more effective antitumor drugs. In this study, we propose that the platelet-derived growth factor receptor-α (PDGFRα)-p70S6K signal transduction pathway in mesenchymal cells, which is required for functional angiogenesis induced by fibroblast growth factor-2, is the potent candidate. Using murine limb ischemia as a tumor-free assay system, we demonstrated that p70S6K inhibitor rapamycin (RAPA) targets mesenchymal cells to shut down the sustained expression of vascular endothelial growth factor (VEGF) and hepatocyte growth factor (HGF), via silencing of the PDGFRα-p70S6K pathway. Irrespective of the varied expression profiles of angiogenic factors in each tumor tested, RAPA constantly led the tumors to dormancy and severe ischemia in the time course, even associated with upregulated expression of VEGF from tumors. Because RAPA showed only a minimal effect to hypoxia-related expression of VEGF in culture, these results suggest that RAPA targets the host-vasculature rather than tumor itself in vivo. Thus, our current study indicates that the PDGFRα-p70S6K pathway is an essential regulator for FGF-2–mediated therapeutic neovascularization, as well as for the host-derived vasculature but not tumors during tumor angiogenesis, via controlling continuity of expression of multiple angiogenic growth factors. **(*Circ Res*. 2004;94:1186-1194.)**

Key Words: tumor ■ angiogenesis ■ mesenchymal cells ■ PDGF-AA ■ p70S6K

Angiogenesis is required for tumor progression, as supported by a number of animal studies demonstrating a reduction in tumor growth by antiangiogenic agents.[1–3] Vascular endothelial growth factor (VEGF) is a key mediator of tumor angiogenesis, and inhibition of VEGF activity by the overexpression of a soluble high-affinity receptor, *fms*-like tyrosine kinase-1 (FLT-1), induced tumor dormancy.[4,5] These studies thus suggest that VEGF-related signaling could be a target for tumor angiogenesis; however, an independent study indicated that the antitumor effect of FLT-1 was highly dependent on the expression level of VEGF in each tumor type studied,[6] suggesting a possible limitation of the anti-VEGF strategy. Therefore, the discovery of common molecular targets of tumor angiogenesis that are independent of the profile of angiogenic growth factor expression in each tumor type would be desirable for the development of broad-acting antitumor agents.

A recent elegant study explored the potential of an immunosuppressive drug, rapamycin (RAPA), which is antiangiogenic; in that study, tumor regression was successfully demonstrated.[7] Although immunosuppressive therapy for patients after organ transplantation promotes the risks of cancer development and recurrence, the use of RAPA or related derivatives was thought to possibly reduce the chance of the development of malignancies. The antiangiogenic effect of RAPA was suggested to involve the reduced expression of VEGF by tumor according to the data from cultured cells[7]; however, its exact mechanism of action in vivo remains unknown.

Independently, we recently demonstrated the critical role of mesenchymal, but not endothelial cell (EC), expression of angiogenic polypeptides during therapeutic angiogenesis using fibroblast growth factor-2 (FGF-2) to treat critical limb ischemia.[8,9] FGF-2 stimulated the local expression of VEGF

Original received November 4, 2003; revision received March 11, 2004; accepted March 22, 2004.

From the Division of Pathophysiological and Experimental Pathology, Department of Pathology (N.T., Y.Y., Y.S., M.O., M.T., S.O., K.K., K.S.), Department of Surgery and Science (N.T., Y.S., M.T., K.K., Y.M.), and Department of Disaster and Emergency Medicine (M. Hashizume), Graduate School of Medical Sciences, Kyushu University, Fukuoka, Japan; DNAVEC Research Inc (M. Hasegawa), Tsukuba, Ibaraki, Japan.

Correspondence to Yoshikazu Yonemitsu, MD, PhD, Division of Pathophysiological and Experimental Pathology, Department of Pathology, Graduate School of Medical Sciences, Kyushu University, 3-1-1 Maidashi, Higashi-ku, Fukuoka 812-8582, Japan. E-mail yonemitu@patho11.med.kyushu-u.ac.jp

Circulation Research **is available at http://www.circresaha.org** **DOI: 10.1161/01.RES.0000126925.66005.39**

and hepatocyte growth factor/scatter factor (HGF/SF), an alternative angiogenic factor, in mesenchymal cells (MCs; including pericytes, vascular smooth muscle cells and adventitial fibroblasts) in the vasculature.[9] Interestingly, the time course of FGF-2–mediated HGF/SF expression was biphasic; early upregulation did not require new protein synthesis, whereas later upregulation was mediated and maintained by endogenous platelet–derived growth factor receptor-α (PDGFRα)- p70S6K pathways.[9]

Because not only VEGF but also host-derived FGF-2 activity is likely to be involved in tumor progression,[10] and also because RAPA is a specific inhibitor of p70S6K via reducing the activity of target of rapamycin (TOR), we hypothesized that the antitumor effect of RAPA might involve the PDGFRα-p70S6K signaling pathway in host-originated stromal MCs, which should be independent of the various angiogenic signals from each tumor. In this study, we provide evidence indicating that RAPA targets stromal MCs rather than tumor cells, thereby turning off the PDGFRα-p70S6K system, and in turn silencing angiogenic signals.

Materials and Methods

Cells and Reagents

All cells used in this study were purchased from American Type Culture Correction. The following intracellular signal inhibitors were used at each of the following concentrations on human smooth muscle cells (HSMCs) and MRC5 cells, as previously described[9]: Ras, Ras-inhibitory peptide (50 μmol/L, Alexis Japan); p70S6K, rapamycin (100 ng/mL, Sigma-Aldrich Japan); PKC, bisindolylmaleimide (100 nmol/L, Sigma); PI3K, wortmannin (120 nmol/L, Sigma); MEK, U0126 (10 μmol/L, Promega K.K.); PKA, PKA-inhibitory peptide (1 μmol/L, Calbiochem); and NF-κB, ALLN (5 μmol/L, Roche *Diagnostics*). Neutralizing antibodies (anti-PDGF-AA and anti-PDGFRα from goat), and control goat IgG were from R&D systems. Stocks of recombinant SeVs (SeV-FGF2 and SeV-luciferase) were prepared as previously described.[8,9] Recombinant SeV-expressing extracellular domain of human PDGFRα was constructed as follows: cDNA fragment (amplicon size=1575 bp) was amplified using synthetic primers with restriction enzyme tag (forward *Bgl*II: 5′-aaAGATCTatggggacttccc-atccggc-3′; reverse *Nhe*I: 5′-ttGCTAGCtcacttgtcatcgtcgtccttgtagtcttcagaacgcagggt-3′), and whole sequence was determined as completely matched to reported sequence (GenBank No. NM006206) by capillary sequencer. The clone was inserted into a template plasmid encoding SeV18+, and SeV-hsPDGFα was recovered as described.[8,9,11] The secretion of soluble human PDGFα via SeV-hsPDGFα was determined by Western blotting (data not shown).

Animals

Male C57BL/6 (6 weeks old) and balb/c *nu/nu* mice (5 weeks old) were from KBT Oriental Co, Ltd (Charles River Grade, Tosu, Saga, Japan). All animal experiments were performed according to approved protocols and in accordance with recommendations for the proper care and use of laboratory animals by the Committee for Animals, Recombinant DNA, and Experiments Using Infectious Pathogen at Kyushu University, and according to The Law (No. 105) and Notification (No. 6) of the Japanese Government.

Limb Ischemia Models

The details of the surgical treatment and evaluation of limb prognosis were described previously.[8,9] For the gene transfer, 25 μL of vector solutions were injected into two portions of the thigh muscle soon after the completion of the surgical procedures. In vivo suppression of endogenous PDGF-AA activity was performed as previously described using PDGF-AA-specific neutralizing goat polyclonal IgG (cross-reactive to human and murine proteins) via a disposable micro-osmotic pump (Model 1007D, ALZA Co) as previously described.[8,9]

Tumor Implantation

For tumor implantation, 10^6 SAS or MH134 cells were intradermally implanted into the abdominal wall, and the tumor volume was evaluated every other day. Seven days after implantation, RAPA (1.5 mg/kg per day) was intraperitoneally administered daily. On day 7 or 28, mice were euthanized, and the tumors were subjected to enzyme-linked immunosorbent assay (ELISA).

Enzyme-Linked Immunosorbent Assay

Protein contents in murine limb muscles, tumors, and culture medium were determined using Quantikine Immunoassay systems for murine (recognizes both 164 and 120 amino acid residue forms) and human VEGF-A, human FGF-2 (available to both human and murine), human HGF (R&D Systems Inc), and rat HGF (available to murine HGF, Institute of Immunology Inc) according to the manufacturer's instructions, as previously described.[8,9]

Northern Blot Analysis

Total cellular RNA, isolated using the ISOGEN system (Wako Pure Chemicals), was electrophoresed and transferred onto a nylon membrane. The filters were hybridized overnight at 60°C with random [α-^{32}P] dCTP-labeled probes. The bands were then visualized and subjected to densitometry using a photoimager.

Real-Time PCR

Total RNA was extracted from ischemic limb muscles with the ISOGEN system followed by RNase-free DNase I (Boehringer). Aliquots of total RNA(25 ng) were reverse-transcribed and amplified in triplicate with the TaqMan EZ RT-PCR kit and a Sequence Detection System, model 7000 (PE Biosystems). The nucleotide sequences of PCR primers and TaqMan probes are listed in the Table. The murine GAPDH control reagents were used as the internal standard. The target quantity was determined from the relative standard curves constructed with serial dilutions of the control total RNA. The expression level of the target gene was normalized by the GAPDH level in each sample.

Laser Doppler Perfusion Images

Intratumor blood perfusion was evaluated using a laser Doppler perfusion image (LDPI) analyzer (Moor Instruments), as previously described.[8,9] To eliminate background noise due to intestinal blood flow, a blue sheet was inserted into the peritoneal cavity just before the measurement. To minimize the data variables due to ambient light and temperature, the LDPI index was expressed as the ratio of intratumor pixels to those in the scrotum.

Statistical Analysis

All data were expressed as mean±SEM and were analyzed by one-way ANOVA with Fisher's adjustment. For the survival analysis, the survival rate, expressed by limb salvage score,[12] was analyzed using Kaplan-Meyer's method. The statistical significance of the survival experiments was determined using the log-rank test, and $P<0.05$ was considered to be statistically significant.

Results

FGF-2 and PDGF-AA Cooperatively Enhance VEGF and HGF/SF Expression via FGF-2–Mediated Upregulation of PDGFRα

To assess the role of PDGF-AA signaling in the angiogenic response of the host vasculature, we first examined the induction of VEGF and HGF via FGF-2 using cultured human MCs (MRC5 and HSMCs) under serum-free conditions. As shown in Figure 1A, FGF-2, but not PDGF-AA stimulated VEGF in the culture medium of MRC5 cells (Figure 1A, left), and inversely, PDGF-AA, but not FGF-2,

Sequences of Primers and Probes Used for Real-Time PCR

Primer Name (Murine)	Sequence
VEGF amplicon size: 137 bp	
VEGF, forward	5′-GCAGGCTGCTGTAACGATGAA-3′
VEGF, reverse	5′-TCACATCTGCTGTGCTGTAGGA-3′
VEGF, hybridization probe	5′-FAM-CATGCAGATCATGCGGATCAAACCTC-TAMRA-3′
HGF amplicon size: 87 bp	
HGF, forward	5′-CAGCAATACCATTTGGAATGGAAT-3′
HGF, reverse	5′-TTGAAGTTCTCGGGAGTGATATCA-3′
HGF, hybridization probe	5′-FAM-CGTTGGGATTCGCAGTACCCTCACA-TAMRA-3′
PDGF-A amplicon size: 125 bp	
PDGF-A, forward	5′-CGTCAAGTGCCAGCCTTCA-3′
PDGF-A, reverse	5′-ATGCACACTCCAGGTGTTCCT-3′
PDGF-A, hybridization probe	5′-FAM-CACTTTGGCCACCTTGACACTGCG-TAMRA-3′
PDGFRα amplicon size: 148 bp	
PDGFRα, forward	5′-GAGCATCTTCGACAACCTCTACAC-3′
PDGFRα, reverse	5′-CCGGTATCCACTCTTGATCTTATTG-3′
PDGFRα, hybridization probe	5′-FAM-CCCTATCCTGGCATGATGGTCGATTCT-TAMRA-3′
GAPDH amplicon size: 117 bp	
GAPDH, forward	5′-CCTGGAGAAACCTGCCAAGTAT-3′
GAPDH, reverse	5′-TTGAAGTCGCAGGAGACAACCT-3′
GAPDH, hybridization probe	5′-FAM-TGCCTGCTTCACCACCTTCTTGATGT-TAMRA-3′

upregulated VEGF in the medium of HSMCs (Figure 1A, right). On the other hand, costimulation using FGF-2 and PDGF-AA demonstrated a synergistic effect as regards both VEGF expression (Figure 1A) and HGF/SF (data not shown), in both types of cell. Similar to MRC-5 cells, a cell line of murine fibroblasts, NIH3T3, also showed synergistic effect of FGF-2 and PDGF-AA on expression of VEGF and HGF (data not shown), indicating that such effect might be a common system in mesenchymal cells irrespective of animal species. Northern blot analyses showed FGF-2–mediated upregulation of PDGFRα transcription in both types of cell (Figure 1B), whereas PDGF-AA did not alter FGFR1 expression (data not shown); these findings suggest that FGF-2 modulates the response to PDGF-AA regarding VEGF and HGF/SF expression in mesenchymal cells via the transcriptional regulation of PDGFRα.

FGF-2–Dependent, Mesenchymal Expression of VEGF and HGF/SF Expression Is Mediated by PDGFRα, Which Can Be Shut by RAPA

In addition to the cooperative effect of FGF-2 and PDGF-AA on VEGF and HGF/SF expression in MCs, we previously found that FGF-2 also enhanced the endogenous expression of PDGF-AA via Ras and p70S6K signaling, which contributed to the sustained expression of HGF/SF in HSMCs.[9] We thus considered the possibility that a similar system might also be seen in the context of VEGF and HGF/SF expression in fibroblasts (MRC5). As also observed in previous studies, it was found that FGF-2 representatively upregulated both the VEGF and HGF/SF proteins, and these effects were abolished by an MEK inhibitor, Ras-inhibitory peptide, and the p70S6K inhibitor (RAPA) (Figure 2A). Repetitive Northern blot analysis of the time course of FGF-2–mediated VEGF expression exhibited the biphasic (at 3 hours and later) upregulation of VEGF (Figure 2B), as previously seen in the case of HGF/SF expression using HSMCs.[9] Early VEGF expression was not affected, but the later/sustained expression was completely diminished by RAPA treatment (Figure 2B). Furthermore, FGF-2–mediated upregulation of VEGF protein was completely abolished by anti-PDGFRα antibody (Figure 2C); a similar finding observed with RAPA (Figure 2A). As the same results were obtained regarding HGF/SF expression (data not shown), the PDGFRα system was suggested to play a critical role in FGF-2–mediated enhancement and continuity of VEGF and HGF/SF expression in MCs.

PDGFRα Plays a Critical Role in the Therapeutic Effect of FGF-2 in Murine Critical Limb Ischemia

To examine the possible cascade-like link of FGF-2-PDGFRα-VEGF/HGF in vivo, we assessed two independent murine models of limb ischemia, namely a "limb salvage model" in C57 BL/6 mice and an "autoamputation model" in balb/c *nu/nu* mice,[8] using SeV-FGF2 in vivo.[8,9,10–15] Overexpression of FGF-2, which was assessed by ELISA (data not shown), resulted in the upregulation of both PDGF-A and PDGFRα mRNA quantitatively assessed by real-time PCR in a limb salvage model (Figure 3A). Similar enhancement of VEGF and HGF/SF expression by FGF-2 was also observed in the same tissue samples; this effect was diminished by anti–PDGF-AA neutralizing antibody, as well as by RAPA treatment (Figure 3B). This effect of RAPA was also confirmed on the protein level (Figure 3C); furthermore, the therapeutic effect of FGF-2 in the autoamputation model was abolished by anti–PDGF-AA antibody and RAPA (Figure

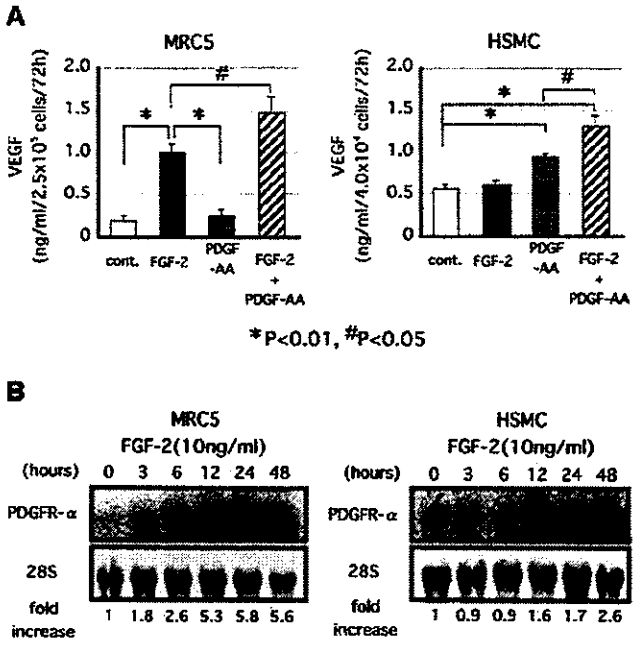

Figure 1. A, FGF-2 and PDGF-AA cooperatively enhance VEGF secretion in fibroblasts (MRC5) and vascular smooth muscle cells (HSMCs). After 48 hours of preincubation without serum, each cell type was stimulated with FGF-2 and/or PDGF-AA. Seventy-two hours later, the culture medium was subjected to ELISA. Each group contained n=3. *P<0.01 and #P<0.05. B, Time course of FGF-2–mediated PDGFRα expression in MRC5 cells and HSMCs (Northern blotting). After 48 hours of preincubation without serum, each cell type was stimulated with FGF-2, and the cells were harvested at each indicated time point. This experiment was performed twice with similar results.

3D), indicating that the PDGFRα system plays a critical role in FGF-2-mediated therapeutic angiogenesis.

RAPA Induces Tumor Dormancy Irrespective of the Variety in the Expression of Angiogenic Factors in Each Type of Tumor

These results from the tumor-free systems suggest that the PDGFRα-p70S6K signal pathway in MCs is essential, and that RAPA imitates the effects of anti–PDGF-AA antibody in FGF-2–mediated angiogenesis. However, an issue arose from this line of questioning regarding whether or not RAPA might be able to affect ubiquitous angiogenic responses, irrespective of angiogenic stimuli. To clarify this issue, we examined tumor angiogenesis using two independent tumor cell lines, ie, SAS-human oral squamous cell carcinoma, which expresses VEGF, FGF-2, and PDGF-AA at high levels; and MH134-murine hepatocellular carcinoma,[16] which secretes far less VEGF and FGF-2 than the former, and shows null expression of PDGF-AA.

RAPA reduced the growth of both tumor types (Figure 4A), indicating that the antitumor effect of RAPA was likely to be independent of the respective expression patterns of angiogenic growth factors in each type of tumor. To obtain further and direct evidence of tumor-independent antitumor effect of PDGFRα-p70S6K pathway, we conducted additional experiments assessing tumor growth via intratumor injection of SeV-hsPDGFRα, which expressed ectodomain of

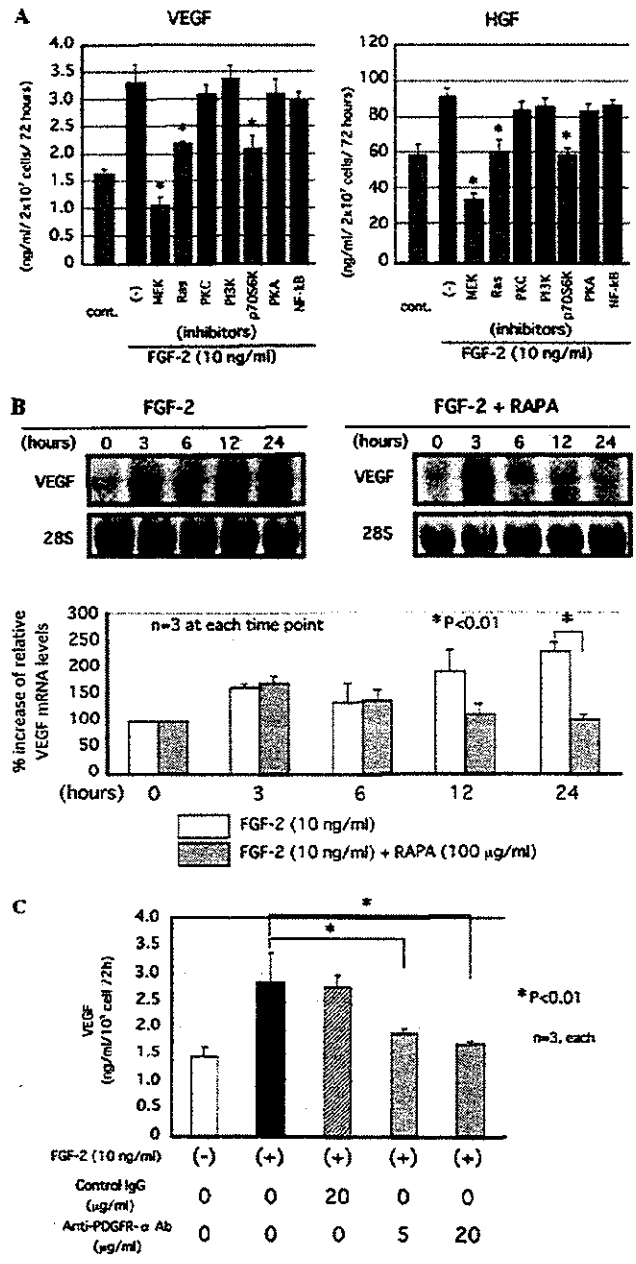

Figure 2. PDGFRα-p70S6K is essential for FGF-2–mediated sustained/biphasic expression of VEGF/HGF in mesenchymal cells. A, Effect of various inhibitors on intracellular signal transduction pathways on VEGF and HGF secretion in MRC5 cells. Forty-eight hours after preincubation with 1% FBS, cells were stimulated by 10 ng/mL of human recombinant FGF-2 with or without various inhibitors. Seventy-two hours later, the medium was subjected to ELISA. Each group contained n=3. *P<0.01. B, p70S6K inhibitor rapamycin (RAPA) abolished the latter phase of FGF-2–mediated VEGF mRNA expression in MRC5 cells. Forty-eight hours after preincubation with 1% FBS, cells were stimulated by 10 ng/mL of recombinant FGF-2. The cells were harvested at each designated time point, and the bands were then visualized and subjected to densitometry using a photoimager. Graph shows the quantitation of relative mRNA levels of VEGF, reflecting the results from triplicate experiments. *P<0.01. C, FGF-2–mediated upregulation of VEGF secretion completely depended on PDGFRα. Forty-eight hours after preincubation with 1% FBS, MRC5 cells were stimulated by 10 ng/mL of recombinant FGF-2 with or without anti-PDGFRα neutralizing antibody. Seventy-two hours later, the culture medium was subjected to ELISA. *P<0.01.

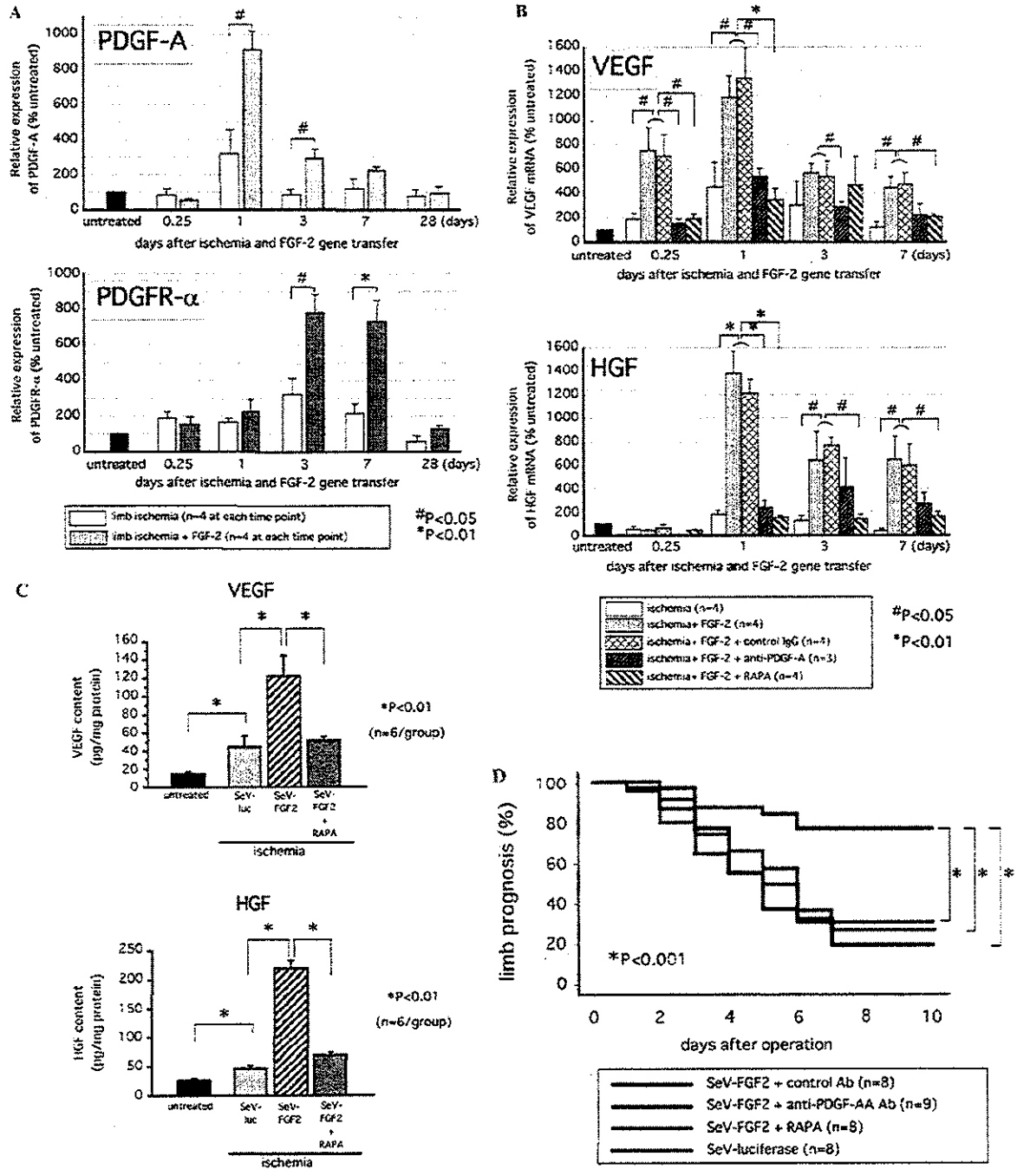

Figure 3. Upregulation of VEGF and HGF is mediated by the PDGFRα system and is essential for the therapeutic effect of FGF-2 gene transfer in murine critical limb ischemia. *$P<0.01$ and #$P<0.05$. A, Time courses of relative PDGF-A (top) PDGFRα (bottom) mRNA expression in ischemic thigh muscles in "limb salvage" model mice with or without FGF-2 gene transfer. Soon after surgery inducing limb ischemia, SeV-mFGF2 (10^7 plaque-forming units, pfu) was injected intramuscularly. At each time point, thigh muscles were subjected to real-time PCR. Data were standardized by each mRNA level of GAPDH and show the relative expression of results obtained from untreated control mice. Each group contained 4 mice. At each time point, one or two control mice with ischemia, which had been injected with control virus (SeV-luciferase), showed similar results to those seen in mice with limb ischemia (data not shown). B, Time courses of relative VEGF (top) and HGF (bottom) mRNA expression in ischemic thigh muscles in "limb salvage" model mice treated with anti–PDGF-AA neutralizing antibody (protocol, see Figure 2D) or RAPA (1.5 mg/kg per day, daily intraperitoneal injection) after FGF-2 gene transfer. Same tissue samples as those shown in Figure 2A from the ischemia and ischemia+FGF-2 groups were used. At each time point, one or two control mice with ischemia, which had also been injected with control virus (SeV-luciferase), showed similar results to those seen in mice with ischemia only (data not shown). C, RAPA inhibited FGF-2–mediated VEGF (top) and HGF (bottom) protein expression in the murine limb ischemia, "limb salvage" model. Intraperitoneal injection of RAPA (1.5 mg/kg per day, daily) was initiated 1 day before day 0, and then surgical ischemia was induced on day 0. At that time, 10^7 pfu of control virus (SeV-luciferase) or SeV-mFGF2 was intramuscularly injected. Two days later, thigh muscles were subjected to ELISA. D, Anti–PDGF-AA neutralizing antibody, as well as RAPA, abolished the therapeutic effect of FGF-2 gene transfer in autoamputation model. Limb prognosis was determined by a limb salvage score of 12, and the data were analyzed by a log-rank test. Anti–PDGF-AA neutralizing antibody was administered by intraperitoneal continuous release (200 μg/7 days) via the implantation of a disposable osmotic pump and by an additional intraperitoneal injection bolus (100 μg) soon after ischemia had been surgically induced.

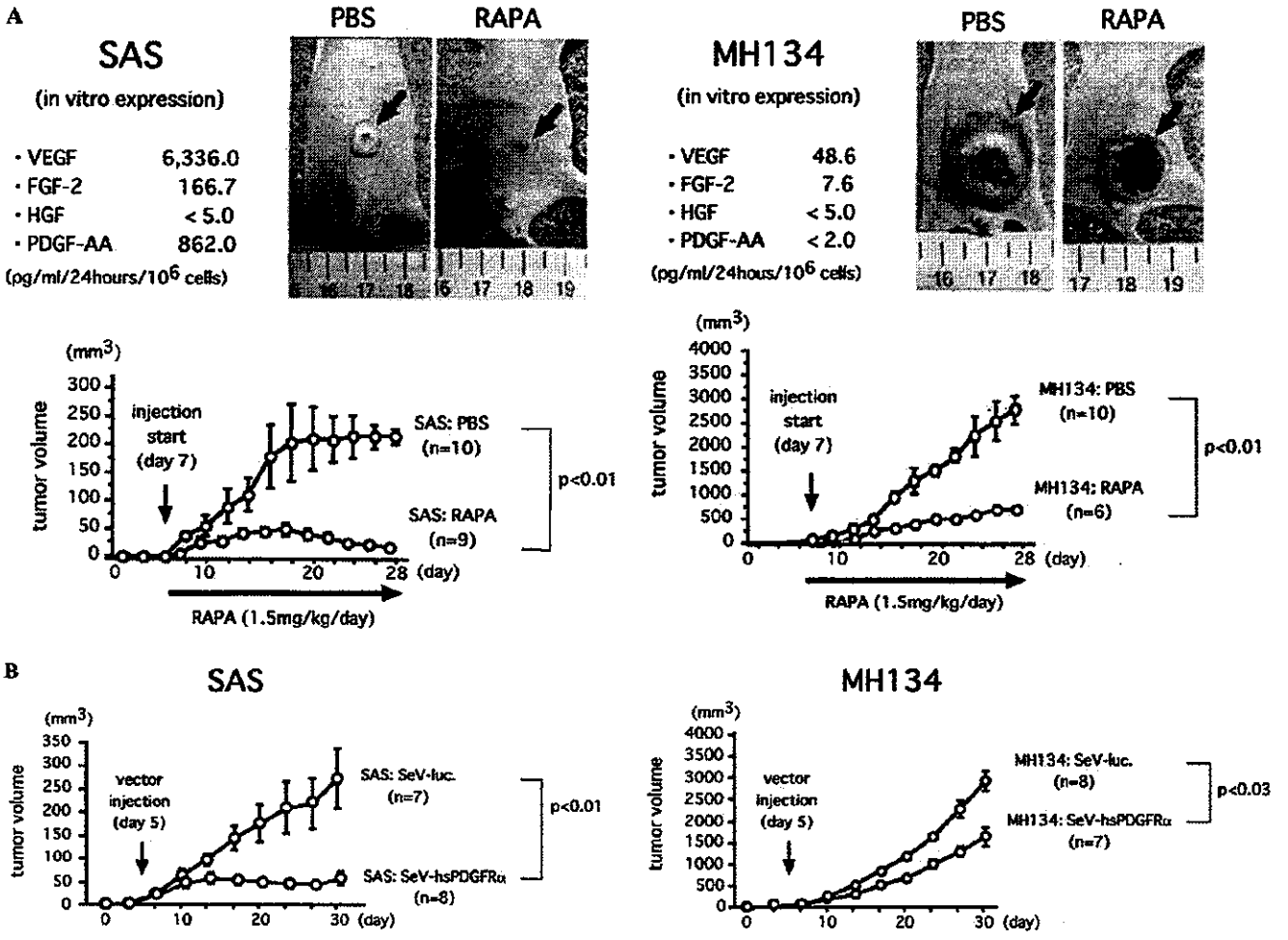

Figure 4. Effects of RAPA treatment on the growth of tumors and on their expression of angiogenic growth factors in vitro and in vivo. Seven days after intradermal implantation of 10^6 cells of each tumor type, daily intraperitoneal injection of RAPA (1.5 mg/kg per day), 0.1 mol/L of phosphate-buffered saline (PBS), or single intratumor injection of SeV-luciferase or SeV-hsPDGFRα (1×10^8 pfu/tumor) was performed. A, In vitro expression patterns of angiogenic growth factors, including PDGF-AA, and the tumor inhibitory effect of RAPA on SAS and MH134. Data include all 3 independent experiments using 2 to 4 mice per experiment. Gross observations were photographed on day 28. Arrows indicate tumors. B, Antitumor effect of recombinant SeV-expressing ectodomain of human PDGFRα on SAS and MH134. Fifty microliters of vector solution was injected intratumorally 5 days after cell implantation. SeV-luciferase was used for control group.

human PDGFRα. As expected, SeV-hsPDGFRα significantly inhibited both tumor types (Figure 4B). Tumor weight was also assessed at the end of experiments, and significantly reduced in both tumors treated with hsPDGFRα compared with luciferase (SAS-luciferase: 415.1±104.9 mg versus SAS-hsPDGFRα=54.3±9.6 mg, MH134-luciferase: 3930.4±304.4 mg versus MH134-hsPDGFRα=2654.4± 296.5 mg, $P=0.0027$ and $P=0.0106$, respectively).

To confirm an interpretation that antitumor effect of RAPA might be independent of the expression pattern of angiogenic factors, we assessed the in vitro and in vivo expression of VEGF with or without RAPA. In culture, 100 ng/mL of RAPA significantly reduced endogenous VEGF secretion approximately 30% to 50% from the SAS baseline, and also from the baseline of the other tumors assessed (squamous cell carcinomas: QG56, TF, KN, EBC-1; and adenocarcinoma: PC9) under normoxia condition; similar findings obtained in the other laboratory.[7] In addition, no effect of RAPA on PDGF-AA and FGF-2 expression was observed in each tumor type (data not shown). In vivo, however, intratumor expressions of VEGF treated with RAPA for 3 or 7 days were significantly upregulated in MH134 tumor compared with those treated with buffer (Figure 5A), and further, Doppler flow image analyses revealed that RAPA reduced blood flow in both tumors on 7 days after the start of RAPA injection (Figure 5B).

These paradoxical results might be explained as follows: RAPA treatment might have induced hypoxia and, as a result, VEGF was upregulated via a hypoxia-dependent mechanism, thereby overcoming the RAPA-mediated downregulation. This hypothesis was also confirmed as follows; RAPA showed significant, but only minimal effect on hypoxia (2.5% O_2)-induced VEGF expression in cultured MH134 (Figure 5C), and similar findings were also obtained in all other cell lines tested (data not shown).

Thus, we next evaluated the source of VEGF in SAS, a xenograft model, using human- and murine-specific ELISA systems. RAPA significantly upregulated human VEGF with-

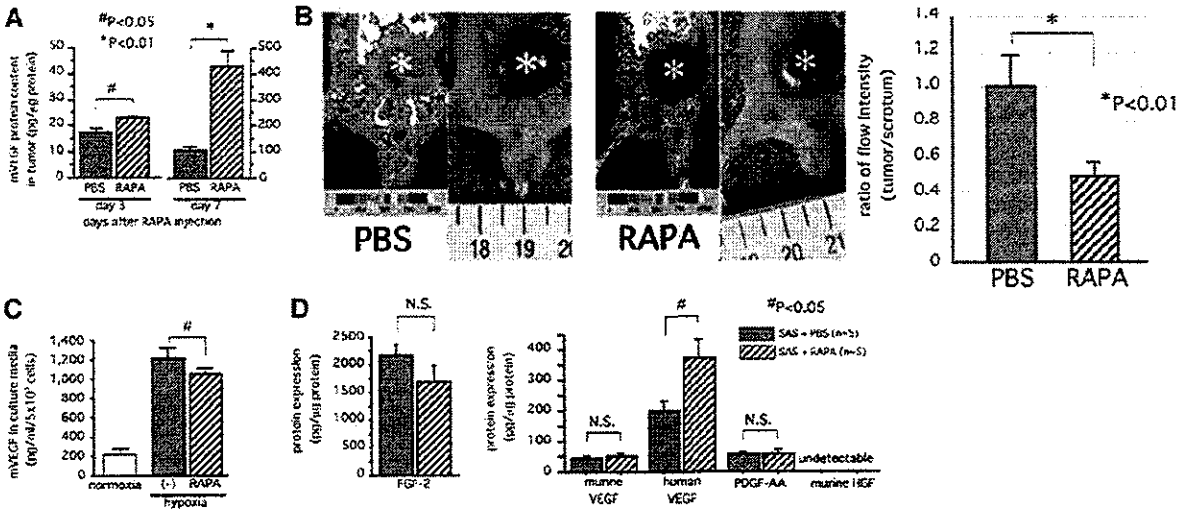

Figure 5. Relationship between tumor blood flow and expression of angiogenic growth factors on MH134 (A through C) and SAS (D). A and B, RAPA-mediated reduction of intratumor blood flow (B, panels and graph) and comparable expression patterns of murine VEGF (A) in vivo. Seven days after the initiation of injections of RAPA to mice bearing syngenic tumors (MH134, asterisks), Doppler flow images were recorded, and then the tumor samples were subjected to ELISA. Tumors on day 3 were also independently subjected to protein measurement (A, on day 3, n=4 at each group). Note that the sizes of the tumors did not significantly different from each other on day 7 (B, asterisks). C, Bar graph indicating the significant, but minimal, effect of RAPA on the hypoxia-induced VEGF expression in MH134 cells. After 12 hours of cultivation under serum-free condition, the cells were washed with fresh medium and exposed to normoxia (21% O_2) or hypoxia (2.5% O_2). Forty-eight hours later, the medium was subjected to ELISA for murine VEGF. D, RAPA-related changes in the expression of angiogenic growth factors in mice bearing a human tumor type (SAS), observed in order to assess the source of upregulated VEGF. Seven days after the initiation of injections of RAPA to mice bearing SAS, the tumor samples were subjected to ELISA systems specific for human or murine VEGF.

out effect to murine VEGF content in solid tumors (Figure 5D), indicating that the upregulation of tumor cell–derived VEGF was mediated by hypoxia due to host vasculature-targeted antiangiogenesis independent to the variation of expression of angiogenic stimuli by each tumor type.

Discussion

In this study, we demonstrated that the PDGFRα signal transduction pathway plays an essential role in MCs, not only in the context of therapeutic treatments, but also as regards tumor angiogenesis, irrespective of the variety in the expression patterns of angiogenic substances in each type of tumor. Thus, the PDGFRα-p70S6K signal transduction pathway in host-derived vasculature was concluded to be a ubiquitous molecular target for inducing tumor dormancy (a scheme representing potential mechanisms is summarized in an online Movie available in the online data supplement at http://circres.ahajournals.org).

The biological role of PDGFRα has been controversial for quite some time. PDGF-AA induces DNA synthesis as well as the proliferation of NIH3T3 cells, but in other cells, it inversely inhibits the chemotactic response induced by other agents.[17] Whereas little evidence is available regarding endothelial expression of PDGF-receptors, PDGF ligands, not only PDGF-AA and -BB, but also -CC, a novel member of PDGF,[18] apparently stimulate in vivo angiogenesis,[19,20] suggesting that other angiogenic stimulators may mediate PDGF-dependent angiogenic processes. Our current study, as well as a previous study,[9] strongly suggest that the PDGFRα system may be critical for the maintenance of angiogenic signals using VEGF and HGF/SF in MCs. However, one limitation of the current study was that it did not include a determination of the PDGF ligands that might be critical during angiogenesis, Because all such ligands can activate PDGFR-α, leading to different cellular responses. Our recent independent study revealed that the neutralization of PDGF-BB also disrupted FGF-2-mediated therapeutic effects in an autoamputation model (Y. Yonemitsu, M. Onimaru, and M. Tanii, unpublished data, 2003), and SeV-hsPDGFRα, which traps both PDGF-AA and -BB, efficiently reduced the growth of SAS in vivo (Figure 4B), suggesting that the cooperative activities of PDGF ligands may be required for the efficient promotion of angiogenesis.

A paradox was observed among the results of this study, namely, that RAPA reduced the FGF-2–mediated upregulation of both VEGF and HGF to those of control levels at hypoxia in limb ischemia (Figure 3C); however, RAPA had no effect on the level murine VEGF in SAS cells with null HGF expression (Figure 5D). A possible explanation for this finding may be as follows: the baseline host MC expression of VEGF and HGF required for tumor angiogenesis in SAS was too low to be detected by ELISA, as endogenous HGF expression was undetectable. These cells in tumor, however, were exposed to hypoxia and thus VEGF was upregulated in hypoxia-dependent manner, irrespective of RAPA treatment. This explanation is reasonable because ischemia-mediated upregulation of VEGF was not affected by RAPA (Figure 3C); furthermore, such an imbalance in the expression levels of VEGF and HGF could disturb the blood flow of neovessels, as shown previously.[9]

We here demonstrated that both RAPA and SeV-hsPDGFRα suppressed tumor growth irrespective of expression profiles of angiogenic growth factors; however, the effect of SeV-hsPDGFRα against MH135 was likely to be

relatively modest compared with that obtained with RAPA (Figures 4A and 4B). The possible explanations were as follows: (1) the expression level of hsPDGFRα was not sufficient during experimental course, because transgene expression of SeV shows its peak at 2 days after gene transfer, and is reduced around 1/10 to 1/100 at 7 days even in nude mice[8]; (2) a possible PDGFRα-independent effect of RAPA, including direct growth inhibition of ECs,[21,22] provided additional antitumor activity in RAPA-treated group; and (3) SAS tumors that have higher levels of PDGF-AA secretion than MH134 are more dependent on PDGF for angiogenesis. The 3rd explanation may be supported by our recent data, indicating that PDGF-AA is also an autocrine regulator for stimulating angiogenic growth factors including VEGF in SAS tumors (Y. Shikada and Y. Yonemitsu, unpublished data, 2004). Ideally, experiments using knockout of PDGF-A allele in mesenchymal cells in vivo might solve this issue; however, it is still difficult to establish such mice at present, because such mice showed lethal phenotype pre- and postnatally.[23]

What is the role of endogenous FGF-2, but not exogenous, in limb ischemia as well as tumor models for angiogenesis? At this time, we do not have any direct data regarding this question, however, some recent observations may be a clue to explain this point. As we previously demonstrated, limb ischemia–mediated upregulation of HGF was significantly and considerably reduced in FGF-2$^{-/-}$ mice compared with that seen in FGF-2$^{+/+}$ mice,[9] and similar findings were found in case of VEGF (Y. Yonemitsu et al, unpublished data, 2003). Furthermore, tumor growth of MH134 was significantly suppressed in FGF-2$^{-/-}$ mice (Y. Yonemitsu and S. Shibata, unpublished data, 2004). Together with these results and a published report by another laboratory, indicating that gene transfer of soluble FGFR1 could effectively reduce tumor growth,[10] it is highly suspected that endogenous FGF-2 may essentially participate in therapeutic as well as tumor angiogenesis in vivo.

Although a number of studies have demonstrated that VEGF is an important angiogenic mediator of tumor growth, the anti-VEGF strategy is likely to depend on the expression levels of VEGF in each tumor type.[6] Other angiogenic switches (eg, HGF/SF, angiopoietin-2, which can be induced by FGF-2[9,24]) may possibly rescue tumor angiogenesis when the VEGF signal is intercepted, because tumor- and/or host-derived FGF-2, for example, is required for the maintenance of tumor vasculature. On the other hand, only the expression level of PDGF-AA in tumors was significantly correlated to the survival of patients with neuroblastomas, even when a high level of expression of various angiogenic factors was detected[25] and further, an inhibitor of PDGFRs is likely to be effective in patients with malignant tumors.[26] More recently, an important study has demonstrated an evidence indicating that a tyrosine kinase inhibitor SU6668 specific for PDGFRs blocked further growth of end-stage tumors in experimental animals, eliciting detachment of pericytes in tumor vasculature, whereas an inhibitor targeting VEGFRs (SU5416) was only effective against early-stage tumors,[27] indicating the requirement of PDGFR signals for the maintenance of tumor growth as well as tumor vasculature. The apparent advance of the current study over these recent reports explored the discovery of an essential pathway downstream of the PDGFRα. Based on these findings, it is thus suggested that an anti-PDGFRα-p70S6K strategy, which can be mimicked by RAPA and abolishes host-derived VEGF and HGF/SF that are required for well-organized tumor vasculature, could be applicable for treatment of a broader range of tumor species than an anti-VEGF system.

No assessment of the contribution of bone marrow–derived stem cells (BM-SCs), which have been shown to contribute to tumor angiogenesis, is a limitation of the current study. Notably, such populations respond to angiogenic growth factors, including FGF-2[28] and VEGF,[29] demonstrating potentials to promote tumor growth. Therefore, further studies are called for to clarify whether PDGFRα-p70S6K system may directly contribute to recruitment of BM-SCs to tumor vasculature.

In conclusion, our current study suggests the utility of a host vasculature–targeted antiangiogenic therapy mediated by the blockade of the PDGFRα-p70S6K signal transduction pathway. Because RAPA itself frequently evokes unfavorable symptoms in the clinical setting,[30] related derivatives or novel compounds targeted the PDGFRα-p70S6K with reduced adverse effects could be unique antitumor agents at a future date.[15,16]

Acknowledgments

This work was supported in part by Grants-in-Aid (Y.Y. and K.S.) from the Japanese Ministry of Education, Culture, Sports, Science, and Technology (12557020, 13307009, and 13877028) and by a Grant of Promotion of Basic Science Research in Medical Frontier of the Organization for Pharmaceutical Safety and Research (Y.Y. and K.S., project No. MF-21). The authors thank Ryoko Nakamura-Hashimoto for her excellent help with the animal experiments.

References

1. Folkman J. Tumor angiogenesis: therapeutic implications. *N Engl J Med.* 1971;285:1182–1186.
2. Holmgren L, O'Reilly MS, Folkman J. Dormancy of micrometastases: balanced proliferation and apoptosis in the presence of angiogenesis suppression. *Nat Med.* 1995;1:149–153.
3. Hlatky L, Hahnfeldt P, Folkman J. Clinical application of antiangiogenic therapy: microvessel density, what it does and doesn't tell us. *J Natl Cancer Inst.* 2002;94:883–893.
4. Goldman CK, Kendall RL, Cabrera G, Soroceanu L, Heike Y, Gillespie GY, Siegal GP, Mao X, Bett AJ, Huckle WR, Thomas KA, Curiel DT. Paracrine expression of a native soluble vascular endothelial growth factor receptor inhibits tumor growth, metastasis, and mortality rate. *Proc Natl Acad Sci U S A.* 1988;95:8795–8800.
5. Kuo CJ, Farnebo F, Yu EY, Christofferson R, Swearingen RA, Carter R, von Recum HA, Yuan J, Kamihara J, Flynn E, D'Amato R, Folkman J, Mulligan RC. Comparative evaluation of the antitumor activity of antiangiogenic proteins delivered by gene transfer. *Proc Natl Acad Sci U S A.* 2001;98:4605–4610.
6. Takayama K, Ueno H, Nakanishi Y, Sakamoto T, Inoue K, Shimizu K, Oohashi H, Hara N. Suppression of tumor angiogenesis and growth by gene transfer of a soluble form of vascular endothelial growth factor receptor into a remote organ. *Cancer Res.* 2000;60:2169–2177.
7. Guba M, von Breitenbuch P, Steinbauer M, Koehl G, Flegel S, Hornung M, Bruns CJ, Zuelke C, Farkas S, Anthuber M, Jauch KW, Geissler EK. Rapamycin inhibits primary and metastatic tumor growth by antiangiogenesis: involvement of vascular endothelial growth factor. *Nat Med.* 2002;8:128–135.
8. Masaki I, Yonemitsu Y, Yamashita A, Sata S, Tanii M, Komori K, Nakagawa K, Hou X, Nagai Y, Hasegawa M, Sugimachi K, Sueishi K. Gene therapy for experimental critical limb ischemia: acceleration of limb

loss by overexpression of VEGF165 but not of FGF-2. *Circ Res.* 2002; 90:966–973.
9. Onimaru M, Yonemitsu Y, Tanii M, Nakagawa K, Masaki I, Okano S, Ishibashi H, Shirasuna K, Hasegawa M, Sueishi K. FGF-2 gene transfer can stimulate HGF expression, irrespective of hypoxia-mediated down regulation in ischemic limbs. *Circ Res.* 2002;91:723–730.
10. Compagni A, Wilgenbus P, Impagnatiello MA, Cotton M, Christofori G. Fibroblast growth factors are required for efficient tumor angiogenesis. *Cancer Res.* 2000;60:7163–7169.
11. Yonemitsu Y, Kitson C, Ferrari S, Farley R, Griesenbach U, Judd D, Steel R, Scheid P, Zhu J, Jeffery PK, Kato A, Hasan MK, Nagai Y, Masaki I, Fukumura M, Hasegawa M, Geddes DM, Alton EW. Efficient gene transfer to the airway epithelium using recombinant Sendai virus. *Nat Biotechnol.* 2000;18:970–973.
12. Masaki I, Yonemitsu Y, Komori K, Ueno H, Nakashima Y, Nakagawa K, Fukumura M, Kato A, Hasan MK, Nagai Y, Sugimachi K, Hasegawa M, Sueishi K. Recombinant Sendai virus-mediated gene transfer to vasculature: a new class of efficient gene transfer vector to the vascular system. *FASEB J.* 2001;15:1294–1296.
13. Yamashita A, Yonemitsu Y, Okano S, Nakagawa K, Nakashima Y, Irisa T, Iwamoto Y, Nagai Y, Hasegawa M, Sueishi K. Fibroblast growth factor-2 determines severity of joint disease in adjuvant-induced arthritis in rats. *J Immunol.* 2002;168:450–457.
14. Shoji F, Yonemitsu Y, Okano S, Yoshino I, Nakagawa K, Nakashima Y, Hasegawa M, Sugimachi K, Sueishi K. Airway-directed gene transfer of interleukin-10 using recombinant Sendai virus effectively prevents post-transplantation fibrous airway obliteration in mice. *Gene Ther.* 2003;10: 213–218.
15. Jin CH, Kusuhara K, Yonemitsu Y, Nomura A, Okano S, Takeshita H, Hasegawa M, Sueishi K, Hara T. Recombinant Sendai virus provides a highly efficient gene transfer into human cord blood-derived hematopoietic stem cells. *Gene Ther.* 2003;10:272–280.
16. Tanaka S, Mori M, Sakamoto Y, Makuuchi M, Sugimachi K, Wands JR. Biologic significance of angiopoietin-2 expression in human hepatocellular carcinoma. *J Clin Invest.* 1999;103:341–345.
17. Siegbahn A, Hammacher A, Westermark B, Heldin CH. Differential effects of the various isoforms of platelet-derived growth factor on chemotaxis of fibroblasts, monocytes, and granulocytes. *J Clin Invest.* 1990; 85:916–920.
18. Li X, Ponten A, Aase K, Karlsson L, Abramsson A, Uutela M, Backstrom G, Hellstrom M, Bostrom H, Li H, Soriano P, Betsholtz C, Heldin CH, Alitalo K, Ostman A, Eriksson U. PDGF-C is a new protease-activated ligand for the PDGF α-receptor. *Nat Cell Biol.* 2000;2:302–309.
19. Nicosia RF, Nicosia SV, Smith M. Vascular endothelial growth factor, platelet-derived growth factor, and insulin-like growth factor-1 promote rat aortic angiogenesis in vitro. *Am J Pathol.* 1994;145:1023–1029.
20. Cao R, Brakenhielm E, Li X, Pietras K, Widenfalk J, Ostman A, Eriksson U, Cao Y. Angiogenesis stimulated by PDGF-CC, a novel member in the PDGF family, involves activation of PDGFR-αα and -αβ receptors. *FASEB J.* 2002;16:1575–1583.
21. Vinals F, Chambard JC, Pouyssegur J. p70 S6 kinase-mediated protein synthesis is a critical step for vascular endothelial cell proliferation. *J Biol Chem.* 1999;274:26776–26782.
22. Yu Y, Sato JD. MAP kinases, phosphatidylinositol 3-kinase, and p70 S6 kinase mediate the mitogenic response of human endothelial cells to vascular endothelial growth factor. *J Cell Physiol.* 1999;178:235–246.
23. Bostrom H, Willetts K, Pekny M, Leveen P, Lindahl P, Hedstrand H, Pekna M, Hellstrom M, Gebre-Medhin S, Schalling M, Nilsson M, Kurland S, Tornell J, Heath JK, Betsholtz C. PDGF-A signaling is a critical event in lung alveolar myofibroblast development and alveogenesis. *Cell.* 1996;85:863–873.
24. Mandriota SJ, Pepper MS. Regulation of angiopoietin-2 mRNA levels in bovine microvascular endothelial cells by cytokines and hypoxia. *Circ Res.* 1998;83:852–859.
25. Eggert A, Ikegaki N, Kwiatkowski J, Zhao H, Brodeur GM, Himelstein BP. High-level expression of angiogenic factors is associated with advanced tumor stage in human neuroblastomas. *Clin Cancer Res.* 2000; 6:1900–1908.
26. George D. Platelet-derived growth factor receptors: a therapeutic target in solid tumors. *Semin Oncol.* 2001;28:S27–S33.
27. Bergers G, Song S, Meyer-Morse N, Bergsland E, Hanahan D. Benefits of targeting both pericytes and endothelial cells in the tumor vasculature with kinase inhibitors. *J Clin Invest.* 2003;111:1287–1295.
28. van den Bos C, Mosca JD, Winkles J, Kerrigan L, Burgess WH, Marshak DR. Human mesenchymal stem cells respond to fibroblast growth factors. *Hum Cell.* 1997;10:45–50.
29. Al-Khaldi A, Eliopoulos N, Martineau D, Lejeune L, Lachapelle K, Galipeau J. Postnatal bone marrow stromal cells elicit a potent VEGF-dependent neoangiogenic response in vivo. *Gene Ther.* 2003;10: 621–629.
30. Brara PS, Moussavian M, Grise MA, Reilly JP, Fernandez M, Schatz RA, Teirstein PS. Pilot trial of oral rapamycin for recalcitrant restenosis. *Circulation.* 2003;107:1722–1724.

Long-Term Treatment With a Rho-Kinase Inhibitor Improves Monocrotaline-Induced Fatal Pulmonary Hypertension in Rats

Kohtaro Abe, Hiroaki Shimokawa, Keiko Morikawa, Toyokazu Uwatoku, Keiji Oi, Yasuharu Matsumoto, Tsuyoshi Hattori, Yutaka Nakashima, Kozo Kaibuchi, Katsuo Sueishi, Akira Takeshita

Abstract—Primary pulmonary hypertension is a fatal disease characterized by endothelial dysfunction, hypercontraction and proliferation of vascular smooth muscle cells (VSMCs), and migration of inflammatory cells, for which no satisfactory treatment has yet been developed. We have recently demonstrated that intracellular signaling pathway mediated by Rho-kinase, an effector of the small GTPase Rho, is involved in the pathogenesis of arteriosclerosis. In the present study, we examined whether the Rho-kinase–mediated pathway is also involved in the pathogenesis of fatal pulmonary hypertension in rats. Animals received a subcutaneous injection of monocrotaline, which resulted in the development of severe pulmonary hypertension, right ventricular hypertrophy, and pulmonary vascular lesions in 3 weeks associated with subsequent high mortality rate. The long-term blockade of Rho-kinase with fasudil, which is metabolized to a specific Rho-kinase inhibitor hydroxyfasudil after oral administration, markedly improved survival when started concomitantly with monocrotaline and even when started after development of pulmonary hypertension. The fasudil treatment improved pulmonary hypertension, right ventricular hypertrophy, and pulmonary vascular lesions with suppression of VSMC proliferation and macrophage infiltration, enhanced VSMC apoptosis, and amelioration of endothelial dysfunction and VSMC hypercontraction. These results indicate that Rho-kinase–mediated pathway is substantially involved in the pathogenesis of pulmonary hypertension, suggesting that the molecule could be a novel therapeutic target for the fatal disorder. (***Circ Res.*** **2004;94:385-393.)**

Key Words: pulmonary hypertension ■ Rho-kinase ■ vascular smooth muscle cells ■ endothelial nitric oxide synthase ■ macrophages

Primary pulmonary hypertension (PPH) is a life-threatening disease characterized by a marked and sustained elevation of pulmonary artery pressure. The disease has no obvious causes and ultimately results in right ventricular (RV) failure and death. The pathological changes of hypertensive pulmonary arteries include endothelial injury, proliferation and hypercontraction of vascular smooth muscle cells (VSMCs), and migration of macrophages.[1–3] PPH continues to be a serious clinical problem with high morbidity and mortality.[4]

In 1990s, Rho-kinase/ROK/ROCK was identified as an effector of the small GTPase Rho,[5–7] which plays an important role in various cellular functions, including smooth muscle contraction, actin cytoskeleton organization, cell adhesion and motility, cytokinesis, and gene expression.[8–10] In a series of experimental and clinical studies, we have demonstrated that Rho-kinase–mediated pathway is substantially involved in the pathogenesis of arteriosclerosis.[11–17] These Rho-kinase–mediated alterations in blood vessels also may be involved in the pathogenesis of pulmonary hypertension (PH). In this study, we examined whether Rho-kinase–mediated pathway is involved in the pathogenesis of rat model of fatal PH in vivo.

Materials and Methods

The present study was approved by the Institutional Animal Care and Use Committee of the Kyushu University Graduate School of Medical Sciences.

Animal Model of Fatal PH

A total of 323 adult male Sprague-Dawley rats (Charles River, Yokohama, Japan; 250 to 300 g body weight) were used, including 156 for survival study, 83 for hemodynamic and histology study, 36

Original received October 31, 2003; revision received November 24, 2003; accepted December 1, 2003.

From the Department of Cardiovascular Medicine (K.A., H.S., K.M., T.U., K.O., Y.M., T.H.) and Pathophysiological and Experimental Pathology (Y.N., K.S.), Kyushu University Graduate School of Medical Sciences, Fukuoka, Japan; Kyushu University COE Program on Lifestyle-Related Diseases (H.S., K.S.), and Department of Cell Pharmacology (K.K.), Nagoya University, Graduate School of Medicine, Nagoya, Japan.

This study was presented at the Pulmonary Circulation Council of the American Heart Association, Chicago, Ill, November 17–20, 2002, and published in abstract form [*Circulation.* 2002;106(suppl II):II-365].

Correspondence to Hiroaki Shimokawa, MD, PhD, Department of Cardiovascular Medicine, Kyushu University Graduate School of Medical Sciences, 3-1-1 Maidashi, Higashi-ku, Fukuoka 812-8582, Japan. E-mail shimo@cardiol.med.kyushu-u.ac.jp

Circulation Research **is available at http://www.circresaha.org** **DOI: 10.1161/01.RES.0000111804.34509.94**

for immunohistochemistry, 25 for organ chamber experiments, 15 for Western blot analysis, and 8 for drug concentration measurement. They received a single subcutaneous injection of saline or monocrotaline (MCT, 60 mg/kg, Wako), which induces severe PH in 3 weeks with a subsequent high mortality rate in rats.[18] For the long-term inhibition of Rho-kinase, we confirmed that repetitive in vivo gene transfer of dominant-negative Rho-kinase to pulmonary arteries is technically difficult and that genetic disruption of Rho-kinase is embryo lethal. Therefore, we used a long-term pharmacological inhibition with fasudil (Asahi Kasei), which we found is metabolized in the liver to a specific Rho-kinase inhibitor hydroxyfasudil after oral administration.[13] Hydroxyfasudil is a specific Rho-kinase inhibitor as its specificity for Rho-kinase is 100 times higher than for protein kinase C and 1000 times higher than for myosin light-chain kinase.[13] Furthermore, among the 16 kinases recently tested, only hydroxyfasudil (10^{-5} mol/L) showed more than 50% inhibition for Rho-kinase (98%).[19] Thus, we consider that hydroxyfasudil is a reasonably selective inhibitor for Rho-kinase.

In the first prevention protocol, animals were injected with MCT with or without concomitant oral treatment with a low-dose (30 mg/kg per day) or a high-dose (100 mg/kg per day) of fasudil.[12] In the second treatment protocol, animals received the two different doses of fasudil, starting at day 21 after MCT injection when severe PH had already been established. In this treatment protocol, hemodynamic parameters were also measured at day 35 in additional animals of the control and the fasudil groups in order to examine those variables before they died.

Hemodynamic Measurements

After the animals were anesthetized with sodium pentobarbital (30 mg/kg, IP), polyethylene catheters were inserted into the RV through the jugular vein and the carotid artery for hemodynamic measurements. RV systolic pressure and systemic blood pressure were measured with a polygraph system (AP-601G, Nihon Kohden).

RV Hypertrophy

The RV was dissected from the left ventricle (LV) and the septum (S) and weighed to determine the extent of RV hypertrophy (RVH) as follows: RV/(LV+S).[18]

Survival Analysis

We examined the effects of fasudil on the survival of MCT-injected rats. The day of MCT injection was defined as day 0. This survival analysis covered the entire experimental period to day 63.

Morphometric Analysis of Pulmonary Arteries

After the hemodynamic measurements, lung tissue was prepared for morphometric analysis by using the barium injection method.[18] All barium-filled arteries of 15 to 50 μm in diameter were evaluated for muscularization of pulmonary microvessels.[18] Arteries of more than 50 μm in diameter were evaluated for measurement of medial wall thickness at a magnification of 400×. For each artery, the median wall thickness was expressed as follows: percent wall thickness=[(medial thickness×2)/external diameter]×100.[18]

Immunohistochemical Analysis

Immunohistochemical analysis was performed at day 21 in the saline-treated control group and the high-dose fasudil group in the prevention protocol. Proliferating cells were evaluated by proliferating cell nuclear antigen (PCNA) staining (Dako) and apoptotic cells by the terminal deoxynucleotidyl transferase (TdT)–mediated dUTP nick end-labeling (TUNEL) method (apoptosis detection kit, Wako). Inflammatory cells were evaluated by ED-1 (analogue of CD68) staining (Santa Cruz Biotechnology). The number of PCNA- and TUNEL-positive cells in 10 fields for each section was quantitatively evaluated as a percent of that of total cells at a magnification of 400× in a blind manner.[18,20] The number of ED-1–positive cells was counted in 30 fields.[3]

Organ Chamber Experiments

Organ chamber experiments were performed at day 21 in the control and the high-dose fasudil groups in the prevention protocol, when MCT-induced PH was established. The extrapulmonary arteries were carefully isolated and cleaned of any connective tissue in physiological salt solution (PSS).[21] The rings from each pulmonary artery (≈1 mm in length) were mounted vertically between two hooks in organ chamber myographs (Medical Supply), which were filled with PSS and kept at 37°C. Isometric tension was measured with force transducers (Nihon Kohden). Each preparation was stretched in a stepwise manner to an optimal length where the force induced by 118 mmol/L KCl became maximal and constant. After equilibration for 30 minutes, endothelium-dependent relaxation to acetylcholine (ACh, 10^{-9} to 10^{-5} mol/L) was examined during a contraction to prostaglandin $F_{2\alpha}$ (3×10^{-6} to 10^{-5} mol/L) in the presence of indomethacin (10^{-5} mol/L) with or without N^{ω}-nitro-L-arginine (L-NNA, 10^{-4} mol/L).[21] Endothelium-independent contractions to serotonin (10^{-9} to 10^{-5} mol/L) and sodium nitroprusside (SNP, 10^{-10} to 10^{-5} mol/L) were also examined in rings without endothelium. The inhibitory effect of acute administration of hydroxyfasudil (10^{-5} mol/L) on the serotonin-induced VSMC hypercontraction was also examined.

Western Blot Analysis

Western blot analysis was performed at day 21 in the control and the high-dose fasudil groups in the prevention protocol. The bilateral pulmonary arteries were isolated and were stabilized in bubbling Krebs solution for 1 hour. These samples were immediately frozen by immersion in acetone containing 10% trichloroacetic acid (TCA) cooled with dry ice, for Western blot analysis of phosphorylations of the ERM (ezrin, radixin, and moesin) family, a substrate of Rho-kinase.[15] ERM is phosphorylated by Rho-kinase at T567 (ezrin), T5648 (radixin), and T558 (moesin).[22] The frozen specimens were washed three times with acetone containing dithiothreitol (10 mmol/L) to remove the TCA and dried. The dried samples were cut into small pieces, exposed to 200 μL of SDS-PAGE sample buffer for protein extraction. The extracted samples (20 μg of protein) were subjected to SDS-PAGE/immunoblot analysis by using the specific ERM antibody.[15] The regions containing ERM family proteins were visualized by ECL Western blotting luminal reagent (Santa Cruz Biotechnology). The extent of the ERM phosphorylation was normalized by that of total ERM. The protein expression of endothelial nitric oxide synthase (eNOS) and β-actin as an internal control in lungs was also analyzed by Western blot analysis.[23–25]

Plasma Concentration of Hydroxyfasudil

We measured plasma concentration of hydroxyfasudil every 6 hours a day in rats that received fasudil in drinking water. We obtained blood samples from carotid arteries in each rat. Plasma concentrations were measured by an HPLC method.[16]

Statistical Analysis

All results are expressed as the mean±SEM. Survival curves were analyzed by the Kaplan-Meier method and analyzed by a log-rank test. Differences in all other parameters were evaluated by ANOVA followed by Fisher's post hoc test. A value of $P<0.05$ was considered to be statistically significant.

Results

Beneficial Effects of Fasudil on Survival

In the control MCT group, survival rate at day 63 was only 27% (n=26) (Figures 1A and 1B). In the prevention protocol, the fasudil treatment markedly and dose-dependently improved the survival at day 63: 77% in the low-dose (n=30) and 94% in the high-dose (n=35) groups (Figure 1A). In the treatment protocol, fasudil again significantly and dose-